DEVELOPMENT OF NUCLEIC ACID COATED NANOPARTICLE BASED
LATERAL FLOW ASSAY FOR E.COLI DETECTION

A THESIS SUBMITTED TO
THE GRADUATE SCHOOL OF NATURAL AND APPLIED SCIENCES
OF
MIDDLE EAST TECHNICAL UNIVERSITY

BY

DOĞA BINGÖL

IN PARTIAL FULFILLMENT OF THE REQUIREMENTS
FOR
THE DEGREE OF MASTER OF SCIENCE
IN
BIOTECHNOLOGY

JUNE 2019

Approval of the thesis:

DEVELOPMENT OF NUCLEIC ACID COATED NANOPARTICLE BASED LATERAL FLOW ASSAY FOR E.COLI DETECTION

submitted by **DOĞA BINGÖL** in partial fulfillment of the requirements for the degree of **Master of Science in Biotechnology Department, Middle East Technical University** by,

Prof. Dr. Halil Kalıpçılar
Dean, Graduate School of **Natural and Applied Sciences** _____

Assoc. Prof. Dr. Can Özen
Head of Department, **Biotechnology** _____

Prof. Dr. Hüseyin Avni Öktem
Supervisor, **Biotechnology, METU** _____

Assoc. Prof. Dr. Mahmut Deniz Yılmaz
Co-Supervisor, **Bioeng. / Konya Food and Agriculture Uni** _____

Examining Committee Members:

Prof. Dr. Ayşen Tezcaner
Engineering Science, Middle East Technical University _____

Prof. Dr. Hüseyin Avni Öktem
Biotechnology, METU _____

Prof. Dr. Füsun Eyidoğan
Education Faculty, Başkent University _____

Assoc. Prof. Dr. Mahmut Deniz Yılmaz
Bioengineering, Konya Food and Agriculture Uni _____

Assist. Prof. Dr. Tahir Bayraç
Bioengineering, Karamanoğlu Mehmetbey University _____

Date: 27.06.2019

I hereby declare that all information in this document has been obtained and presented in accordance with academic rules and ethical conduct. I also declare that, as required by these rules and conduct, I have fully cited and referenced all material and results that are not original to this work.

Name, Surname: Doğa Bingöl

Signature:

ABSTRACT

**DEVELOPMENT OF NUCLEIC ACID COATED NANOPARTICLE BASED
LATERAL FLOW ASSAY FOR E.COLI DETECTION**

Bingöl, Doğa
Master of Science, Biotechnology
Supervisor: Prof. Dr. Hüseyin Avni Öktem
Co-Supervisor: Assoc. Prof. Dr. Mahmut Deniz Yılmaz

June 2019, 93 pages

Foodborne diseases have been a serious issue for all societies since the beginning of humanity. Thousands of people suffer from foodborne diseases (FBD) every year according to WHO. These diseases are important due to their high frequency and the expenditures that they affect community negatively. Both developing and developed countries can be affected from large outbreaks of FBD. Although most strains of *Escherichia coli* are beneficial for host microbiota, some serotypes can lead to serious foodborne illnesses in their host. O157:H7 is one of the most virulent strains of *E.coli* and fast detection of *E.coli* O17:H7 is a fundamental aim to help raise the food safety and diminish outbreaks globally.

Recently, nanoparticle based biosensors have drawn attention of scientists because of their quickness, easiness, sensitivity and specificity. The popularity of system composed of target aiming controlled release of cargo has dramatically increased over the past few years. In this study, a novel Probe-gated system was assessed for the detection of eaeA target gene. In the presence of target, cargo is delivered selectively from the pores of nanoparticles.

In this study, hybridization was triggered to detect target oligonucleotide designed from *eaeA* gene which is found in *E.coli* O17:H7. Single stranded probe oligonucleotide with perfect matching for *eaeA* target was used to cap 3,3',5,5'-Tetramethylbenzidine (TMB) loaded silica nanoparticles. As a result of hybridization between probe and target, horseradish peroxidase (HRP) and hydrogen peroxide (H_2O_2) can oxidize TMB which was liberated. Optimization studies were done in order to obtain proper colorimetric reaction on LFA. Therefore, target concentration could be selectively sensed by probes until it was 7.5 µM.

Keywords: Lateral Flow Assays, Biosensors, E.coli, Silica Nanoparticle

ÖZ

E.COLI TANISI İÇİN NÜKLEİK ASİT KAPLANMIŞ SİLİKA NANOPARÇACIK TABANLI YATAY AKIŞ TESTİNİN GELİŞTİRİLMESİ

Bingöl, Doğa
Yüksek Lisans, Biyoteknoloji
Tez Danışmanı: Prof. Dr. Hüseyin Avni Öktem
Ortak Tez Danışmanı: Doç. Dr. Mahmut Deniz Yılmaz

Haziran 2019, 93 sayfa

Gıda kaynaklı hastalıklar, insanlığın başlangıcından beri tüm toplumlar için ciddi bir problem oluşturmaktadır. Dünya Sağlık Örgütü'ne göre her yıl binlerce insan gıda kaynaklı hastalıklardan (FBD) muzdariptir. Bu hastalıklar, sık görülmeleri ve maliyetleri nedeniyle toplumu olumsuz etkler. Hem gelişmekte olan hem de gelişmiş ülkeler gıda kaynaklı büyük salgınlardan etkilenebilir. Çoğu *E.coli* suşu konak mikrobiyotası için faydalı olsa da, bazı serotipler konaklarında ciddi gıda zehirlenmesine neden olabilir. O157: H7, *E.coli*'nin en virülent soylarından biridir ve *E.coli* O17:H7 nin hızlı tespiti, gıda güvenliğini artırmak ve küresel salgınları en aza indirmek için önemli bir adımdır.

Son zamanlarda, nanoparçacık tabanlı biyosensörler, çabukluk, kolaylık, duyarlılık ve özgüllükleri nedeniyle bilim insanlarının dikkatini çekmektedir. Yükün kontrollü bir şekilde tahliye edilmesini amaçlayan hedeflerden oluşan sistemin popülaritesi son birkaç yılda önemi ölçüde artmıştır. Bu çalışmada eaeA genini saptayabilen prob ile kaplı özgün bir sistem incelenmektedir. Hedef varlığında, kargo nanoparçacıkların gözeneklerinden seçici bir şekilde iletilir.

Bu çalışmada, *E.coli* O157:H7'de bulunan *eaeA* geninden tasarlanan hedef oligonükleotidi tespit etmek için hibridizasyon amaçlanmıştır. hedefi için mükemmel uyumu olan tek sarmallı prob oligonükleotidi, 3,3 ', 5,5'-Tetrametilbenzidin (TMB) yüklü silika nanopartikülleri kaplamak için kullanıldı. Prob ve hedef arasındaki hibridizasyonun bir sonucu olarak, TMB ortama salınmış ve HRP-H202 tarafından oksitlenmiştir. LFA üzerinde uygun kolorimetrik reaksiyonun elde edilmesi için optimizasyon deneyleri yapılmıştır. Sonuç olarak, hedef konsantrasyon 7.5 µM olana kadar, hedef tümleyici problar tarafından selektif olarak algılanabilir.

Anahtar Kelimeler: Lateral Akış Testi, Biyosensörler, E.coli, Silika Nanoparçacık

To my mother

ACKNOWLEDGEMENTS

.

TABLE OF CONTENTS

LIST OF TABLES

LIST OF FIGURES

FIGURES

LIST OF ABBREVIATIONS

ABBREVIATIONS

APS: 3-aminopropyl trimethoxysilane

CdS: Cadmium Quantum Dots

CDC: Centers for Disease Control and Prevention

DNA: Deoxyribonucleic acid

AuNPs: Gold Nanoparticles

eaeA : Attachment and Effacing gene

ELISA: Enzyme-Linked ImmunoSorbent Assay

HF: Hi-Flow

HRP: Horseradish Peroxidase

HUS: Hemolytic Uremic Syndrome

LFAs: Lateral Flow Assays

LFIA: Lateral Flow Immunoassay

LBA: Luria Bertani Agar

LBB: Luria Bertani Broth

LoD: Limit of Detection

MSP: Mesoporous

MSP-SiNPS: Mesoporous Silica Nanoparticles

PCR: Polymerase Chain Reaction

PBS: Phosphate Buffer Saline

PoC: Point of Care

QDs: Quantum Dots

RNA: Ribonucleic acid

SI: Signal Intensity

SiNPs: Silica Nanoparticles

Ss: Single stranded

TMB: 3,3′,5,5′-Tetramethylbenzidine

TRH: Thyrotropin-Releasing Hormone

UTIs: Urinary Tract Infections

WHO: World Health Organization

CHAPTER 1

INTRODUCTION

1.1. Foodborne Disease

Foodborne diseases also known as foodborne illnesses are infections caused by food or water contaminated by parasites, bacteria, viruses, chemicals and toxins. The symptoms of foodborne diseases can be mild such as nausea, vomiting and diarrhea but they can also be lethal like neural and brain disorders, hemolytic uremic syndrome (HUS), hemorrhagic colitis poisoning, absenteeism, meningitis, bloody diarrhea, and also premature deaths (Yeni, Yavaş, Alpas, & Soyer, 2016). Food borne diseases are now seems to be the generally accepted as one of the major global public health problems, because every year thousands of people get sick or even die from food-borne illnesses (Figure 1.1). Besides, apart from their individual effects of foodborne diseases, they have a significant impact on socio-economic development of countries. However, many outbreaks caused by food poisoning and their global consequences have not precisely known. Because, analyzing and management of foodborne disease outbreaks require multi-disciplinary work which need knacks for special areas such as clinical medicine, epidemiology, microbiology and chemistry, risk communication and management. The World Health Organization (WHO) announced a first estimate of the worldwide effects of foodborne diseases (World Health Organization, 2015). According to data, there are known thirty-one foodborne disease agents causing 32 diseases. Moreover, these 31 agents ended with 600 million foodborne diseases and 420,000 deaths in 2010 (World Health Organization, 2015). Besides, burden of FBD are especially widespread among children under five years old and individuals live in undeveloped countries. However, these findings are not completely reliable, and more studies are required in order to indicate the real size of the problem (Figure 1.2).

1

The number of deaths caused by foodborne diseases each year in six different regions of the world

- Southeast Asian region
- African region
- Western Pacific region
- Eastern Mediterranean region
- Region of the Americas
- European region
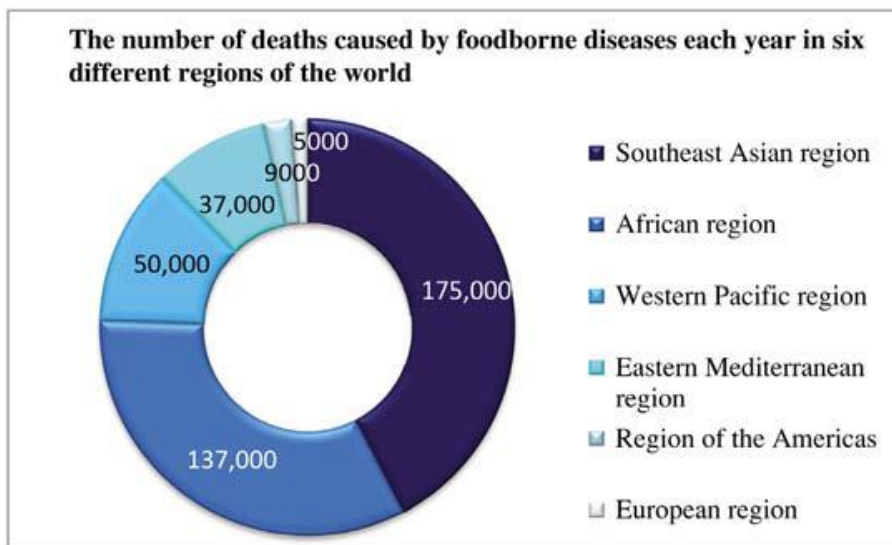
Figure 1.1 Global Burden of Foodborne Diseases—2015 (Ünüvar, 2018) (WHO, 2015).

Reported cases — What we know...
Laboratory tests for organisms
Specimens obtained
Infected persons seek health care
Infected persons (symptomatic)
Infected persons (symptomatic& asymptomatic)
Disease Burden
Exposure of the general population (infected & non-infected) — What we need to know !

Figure 1.2 Stakeout of Foodborne Diseases (Havelaar et al., 2013)

2

1.2. Food Pathogens

1.2.1. Common Bacterial Foodborne Pathogens

Major bacterial foodborne pathogens were mentioned in Table 1.1. As far as fresh produce is concerned, Shigella spp, *Salmonella* spp, Yersinia spp, pathogenic *Escherichia coli*, *Listeria monocytogenes*, Clostridium spp, *Staphylococcus aureus* gain importance.

Table 1.1 Major bacterial foodborne pathogens and clinical features (Yeni et al., 2016)

FOODBORNE PATHOGENS		
Salmonella Species	facultatively anaerobic, non-spore forming, rod-shaped and usually motile	Non typhoidal salmonellosis and typhoid fever
Shigella Species	nonmotile, non-spore forming, rod-shaped	Diarrhea, bacillary dysentery or enterotoxin/ shigatoxin related HUS
Pathogenic *Escherichia coli*	Non-spore-forming, short, facultative anaerobe, rod-shaped	Diarrhea, HUS
Yersinia Species	rod-shaped	diarrhea, abdominal pain, fever, vomiting, and bloody diarrhea in humans
Staphylococcus aureus	spherical, facultative anaerobic, and nonmotile	food poisoning

Listeria monocytogenes	rod-shaped, facultative, non spore-forming, motile	Sepsis, Muscle aches, diarrhea, meningitis, and miscarriage in pregnants
Clostridium Species	anaerobic, rod-shaped, spore-forming	watery diarrhea, botulism in humans

1.2.1.1. *Escherichia coli* O157:H7

Most *E. coli* strains are thought harmless to their hosts since they can naturally colonize and survive in the gut of humans. However, some strains of *E.coli* may obtain mobile genetic elements like plasmids and bacteriophages and as a result they become very dangerous pathogens. These pathogenic *E.coli* are causes of several diseases like diarrhea, neonatal meningitis, septicemia, and urinary tract infections (UTIs) (Makvana & Krilov, 2015) worldwide. *E.coli* is a fecal-oral pathogen and consequently they are usually found in soil and water. According to a study of 90 outbreaks that happened in Canada, Japan, UK, Norway, Ireland, USA, Denmark, and Finland between 1982 and 2006, indicated that the source of transmission was food with 42.2%, dairy compounds with 12.2%, animal interaction with 7.8%, water with 6.7%, from nature with 2.2%, and unknown with 28.9%. Furthermore, various foods and dairy products have been considered as a vector (Figure 1.3).
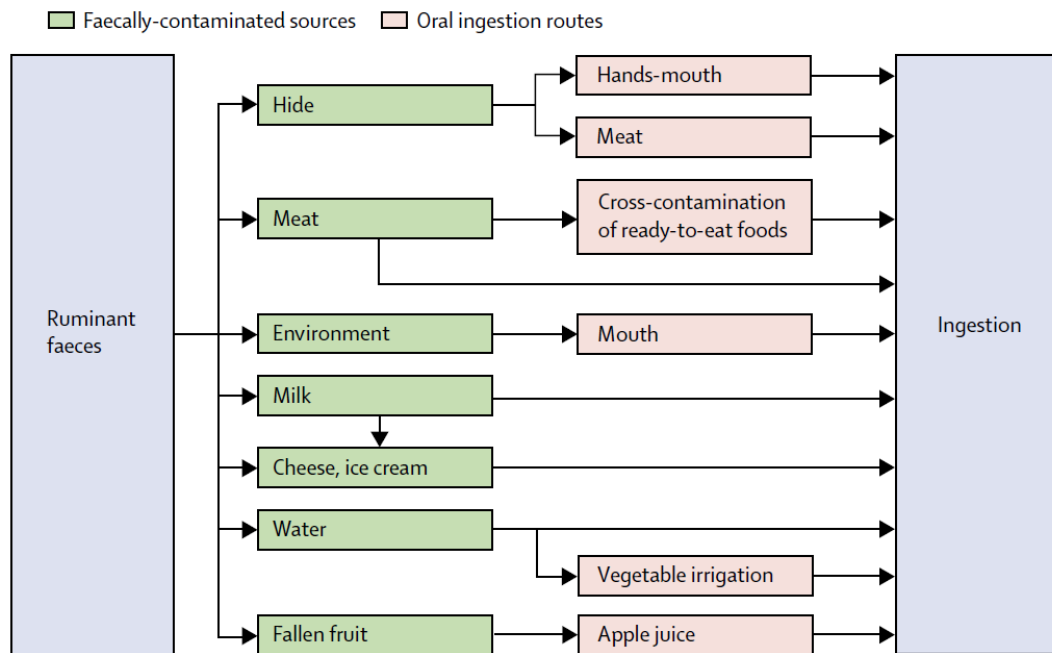
Figure 1.3 Transmission of E.coli O157:H7 (Pennington, 2010)

There are five important *E.coli* pathotypes that differ in their virulence factors, bacterial attachment category to host cells, effects of attachment on host cells, production of toxins, and invasiveness (Yang, Lin, Aljuffali, & Fang, 2017). These are: enterotoxigenic E. coli (ETEC), enteropathogenic *E. coli* (EPEC), Shiga toxin-producing *E. coli*/enterohemorrhagic *E. coli* (STEC/EHEC), *Shigella*/entero invasive *E. coli* (EIEC), enteroaggregative E. coli (EAEC), and (Table 1.2).

Table 1.2 Features of the foodborne pathogenic E. coli (Yang et al., 2017)

Pathotype	Host(s)	Infectious dose (cfu)	Clinical symptoms	Main virulence factors/gene	Virulence associated plasmid	Site of colonization
EPEC	Children <5 year, adults at high inocula	10^8–10^{10}	Watery diarrhea, vomiting, fever, abdominal pain and nausea	LEE, Intimin (eae^+), BFP ($bfp^{+/-}$)	pEAF	Small intestine
STEC/EHEC	Adults, children	<1000	Watery diarrhea, HC and HUS	hemolysin (hly), $eae^{+/-}$, stx^+, $ehxA^+$	pO157 encoding toxins	Distal ileum, colon
EIEC/*Shigella*	Children <5 year, adults, immunocompromised persons, travelers	EIEC: 10^6–10^8 *Shigella*: 10-100	Shigellosis/bacillary dysentery, watery diarrhea, potential HUS	ShET1, ShET2, ial^+, $ipaA,B,C,D,H^+$, sts^+ (*S. dysenteriae*)	Virulence/invasion plasmid (pINV)	Colon
EAEC	Adults, children children in developing countries, travelers	10^{10}	Persistent diarrhea, HUS,	ShET1, ShET2, Pet, $aggR^+$, AAF/I ($aggA^+$) AAF/II ($aafA^+$), AAF/III ($agg3A$), AAF/IV ($agg4A$), AAF/V ($agg5A$) EAST1($astA^+$), dispersin (aap^+)	pAA encoding adherence factors and toxins	Small intestine, colon
ETEC	Children <5 year, adults, immunocompromised persons, travelers	10^8	Watery diarrhea	CFs, LT, ST	Plasmids encoding colonization factors and toxins	Small intestine

Escherichia coli O157:H7 (Figure 1.4) is the most important EHEC serotype regarding community health because it was responsible for foodborne disease outbreaks worldwide. EHEC O157:H7 has gradually originated from non-toxigenic sorbitol-fermenting EPEC O55:H7. When O55:H7 gained the Stxs gene (stx1 or stx2) or virulence associated plasmid (pO157), it cannot ferment sorbitol and turn into O157:H7 strain (Pennington, 2010).
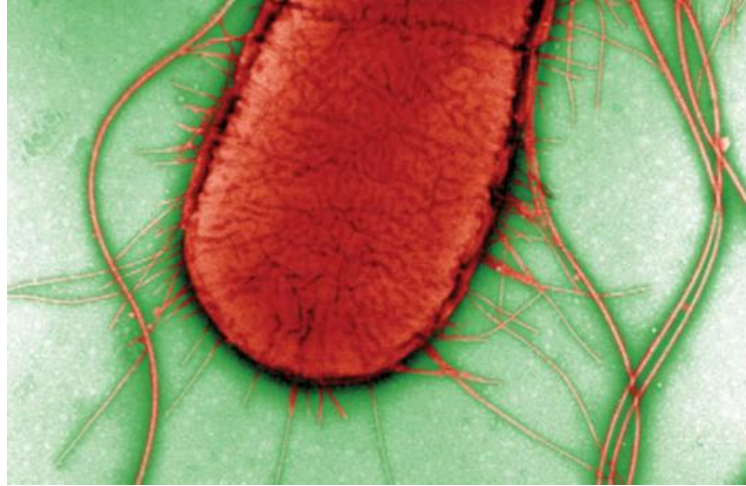
Figure 1.4 An E.coli O157 isolated from the 1996 Central Scotland outbreak Magnification ×50 000 (Pennington, 2010)

E.coli O157 was first known with the outbreaks happened in Oregon and Michigan, USA, in 1982 and UK in 1983 (Pennington, 2010). According to investigations of Centers for Disease Control and Prevention (CDC), the last known multistate outbreak of *E.coli* O157:H7 linked to Romaine Lettuce in the United States. There were 210 people infected in 36 states; 96 people were hospitalized, 27 people developed hemolytic uremic syndrome (HUS), 5 people died (CDC, 2018). It was accepted the worst outbreak of *E.coli* O157:H7 since a 2006 outbreak related with spinach (CNN,2018). Other reports of outbreaks happened in the United States are summarized in Table 1.3 with their case count, hospitalizations, deaths and date.

Table 1.3 Reports of outbreaks of E.coli O157:H7 between 2006-2018 in the United States (CDC,2018)

Source of Outbreak	Case Count	Hospitalizations	Deaths	Date
Romaine Lettuce	210	96	5	2018
Leafy Greens	25	9	1	2017
I.M. Healthy SoyNut Butter	32	12	0	2017
Beef Products	11	7	0	2016
Jack & The Green Sprouts Alfalfa Sprouts	11	2	0	2016
Costco Rotisserie Chicken Salad	19	5	0	2015
Ground Beef	12	58	0	2014
Ready-to-Eat Salads	33	7	0	2013
Organic Spinach and	33	13	0	2012

Spring Mix Blend				
Romaine Lettuce	49	33	0	2011
Lebanon Bologna	13	3	0	2011
In-shell Hazelnuts	8	4	0	2011
Bravo Farms Cheeses	38	15	0	2010
Beef from National Steak and Poultry	21	9	0	2010
Beef from Fairbank Farms	26	19	2	2009
Beef from JBS Swift Beef Company	23	12	0	2009
Prepackaged Cookie Dough	72	34	0	2009
Beef from Kroger/Nebraska Ltd	49	27	0	2008

Totino's/ Jeno's Pizza	21	8	0	2007
Topp's Ground Beef Patties	40	21	0	2007
Taco Bell	71	53	0	2006
Fresh Spinach	199	102	3	2006

The time interval between the individual's disease and the confirmation that he/she is part of an outbreak is generally about 2-3 weeks (Figure 1.5). Therefore, the exact number of all ill people must be more since all individuals who are infected with STEC do not need medical care.
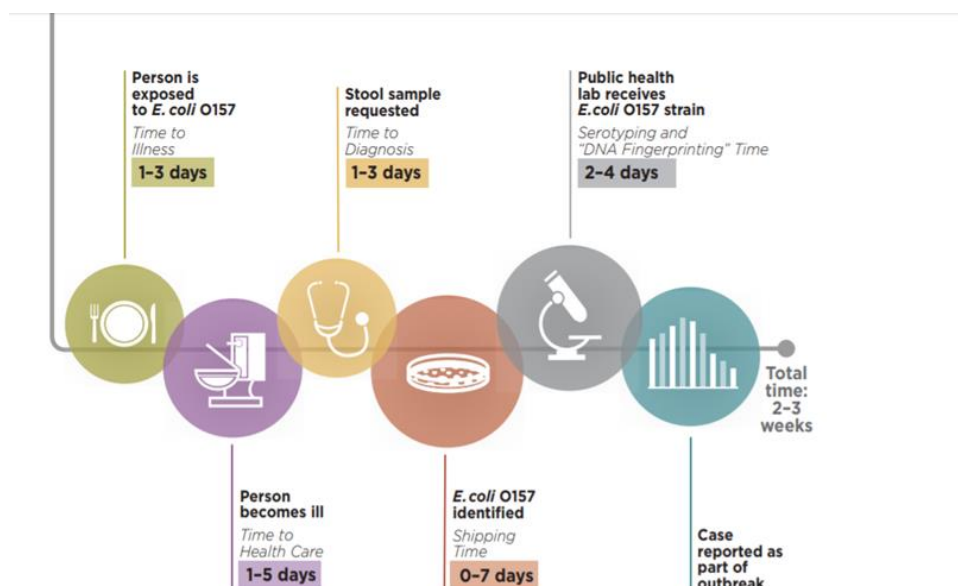
Figure 1.5 Timeline for reporting cases of E. coli O157 Infection (Center for Disease Control and Prevention, 2018)

1.2.1.1.1. eaeA gene

There are several essential bacterial components for intimate binding of EPEC and EHEC to epithelial cells of their hosts. Intimin, which is one of them, is the 94 kDa outer membrane protein encoded by *eaeA* gene. This protein is necessary for the formation of attaching and effacing (A/E) lesion which is fundamental factor for the colonization of EPEC and EHEC in the gut mucosa (Cepeda-Molero *et al*., 2017) (Mckee & O'Brien, 1996). In most of the studies, E. coli has been detected by using *eaeA* gene (Donnenberg *et al*., 1993) (Sandhu *et al*., 1996) (Kiliç, Ertaş, Muz, Özbey, & Kalender, 2007) (Godambe, Bandekar, & Shashidhar, 2017).

1.3. Detection Methods for Foodborne Pathogens

There are several methods employed for food pathogen detection (Figure 1.6).
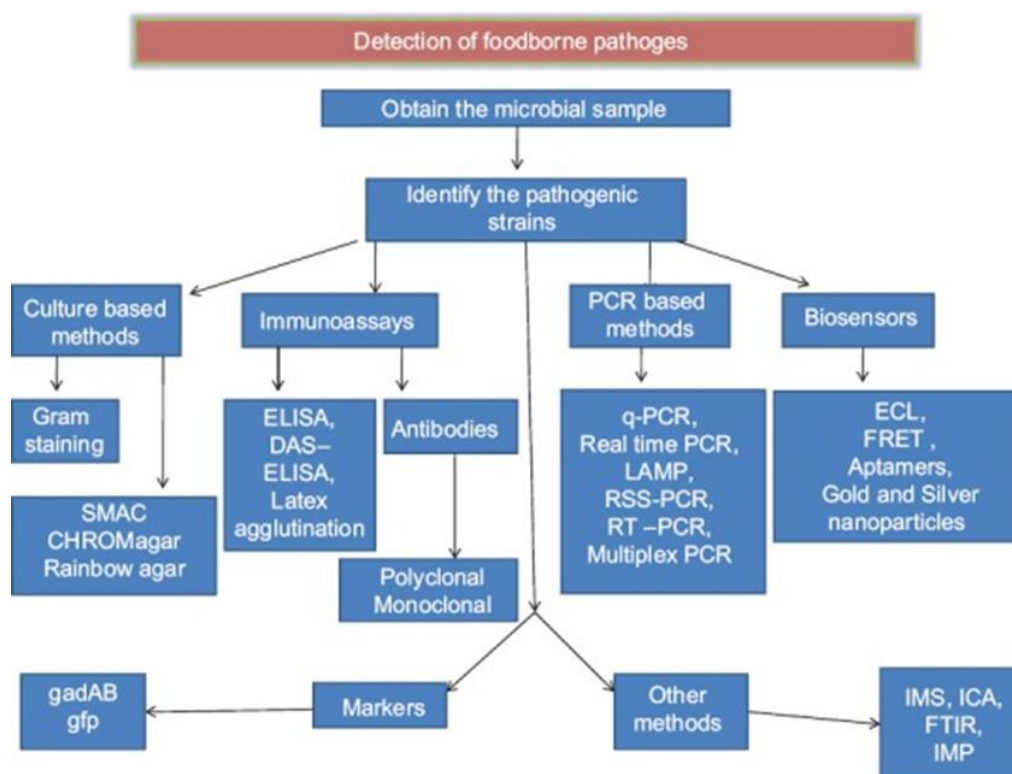
Figure 1.6 Schematic diagram for the detection of foodborne pathogens (Priyanka, Patil, & Dwarakanath, 2016)

1.3.1. Culture-based Methods

Culture based methods have been known to be the oldest detection techniques and they are still accepted as the "gold standards" because of their cost-effectiveness and sensitivity. Moreover, they can provide many information about the feature and number of microorganisms found in food (Baraketi, Amina & Salmieri,2018)

Culture based methods are composed of four main steps which are cultural enrichment, selective and differential plating, and strain typing. Both cultural enrichment and planting steps are done for simple detection and result with exponential amplification and isolation of desired organism respectively. The biggest handicap of culture based method is long duration because each of these steps take between 24 to 48 hours which indicates obtaining positive results can take one week or more with probable detection (Dwivedi & Jaykus, 2011).

Culture can be identified with both qualitatively and quantitatively. In qualitative culture method, it is only considered the presence or absence of microorganisms in the sample. However, in quantitative one enumeration is important and done by plate count method or most probable number method (Stannard, 1997; Betts and Blackborn, 2009; Blodgett, 2010)

Despite traditional culture methods have been recognized as "gold standard" and still preferred for many studies they are cumbersome and time-consuming. Besides, they can give false positive results because of viable but nonculturable (VBNC) cells (Baraketi, Amina & Salmieri,2018)

1.3.2. Alternative Methods

1.3.2.1. Immunological-based methods

Immunological-based methods have been known as rapid, inexpensive and easy to perform. However, they are less specific and less sensitive compared to nucleic acid based methods (Iqbal *et al*., 2000). Success of immunological-based methods depends on the antigen-antibody interaction. At this point, purity and specificity of antibody play a critical role in the reliability of assay (Priyanka *et al*., 2016). Polyclonal and monoclonal antibodies are used in order to perfom immunoassays. Despite being laborious and expensive compared to polyclonal antibodies, monoclonal antibodies are more sensitive and specific to their antigens as they have monovalency (Priyanka

et al., 2016). On the other hand, polyclonal antibodies have polyvalency which means more than one epitope to react with, and this can result with false positive results.

One of the most outstanding immunoassays is Enzyme Linked Immunosorbent Assay (ELISA) during the determination of food pathogens. In ELISA, the antigen from enriched medium is captured by an antibody bound to a solid matrix. When the antigen is immobilized, antibody which form a complex with the antigen is added. Then, bound target is seen by the adding of a chemiluminescent, chromogenic or fluorescent enzyme substrate (Valderrama *et al.*, 2016). Figure 1.7 represents the simplified diagram of ELISA. For instance, pathogenic *Vibrio parahaemolyticus* in seafood was detected with sandwich ELISA using monoclonal antibodies against the TDH-related hemolysin (TRH) of these pathogens (Kumar, Raghunath, Devegowda, & Kumar, 2011). Another frequently employed immunological method for foodborne pathogen detection is lateral flow immunoassay. Figure 1.8 illustrates lateral flow immuno assay. First enriched sample that contain analyte of interest is loaded on reagent pad. After sample is migrated through the assay by the force of capillary action, it encounters with antibodies conjugated to colored particles and specific for target found in the sample. Consequently, analyte is immobilized in capture zone by anti-target analyte antibodies. In the presence of specific antigens, two visible lines (one of them is control line) are observed on lateral flow assay and this means positive result (Valderrama *et al.*, 2016).
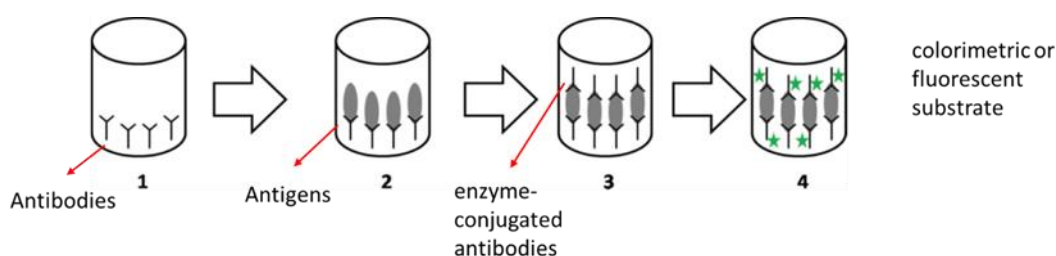
Figure 1.7 Simplified figure of an immunologically based method, ELISA (Valderrama et al., 2016).

14
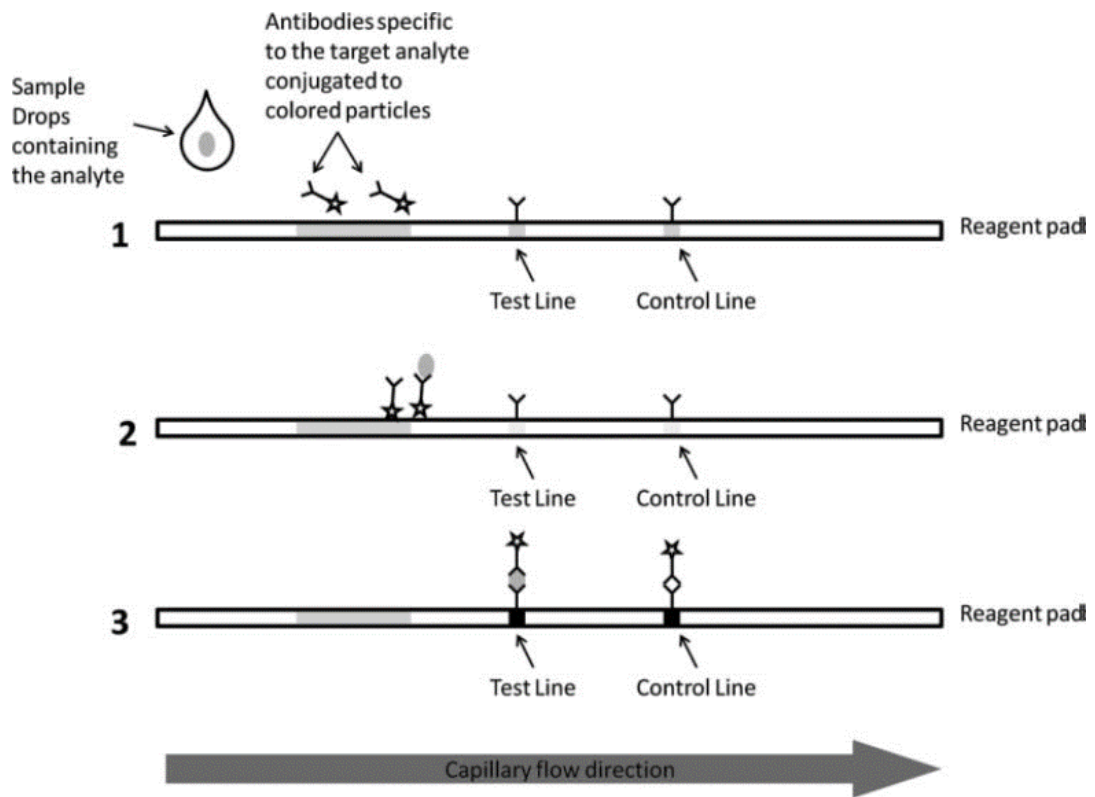
Figure 1.8 Simplified diagram of the lateral flow immunoassay (1) Enriched sample is sent through the reagent pad. (2) Sample travels along the reagent pad and binds to conjugated antibodies. (3) Positive result is obtained when two visible (analyte and control) lines occur (Valderrama et al., 2016).

Lateral flow immune assays are commonly used for the detection of pathogens by combining different strategies such as simultaneous detection of *E.coli* O157:H7 and *Shigella boydii* in jelly product, milk and bread (C. Song *et al*., 2016); methicillin-resistant Staphylococcus aureus in pork (Hongwei Zhang *et al*., 2017) and *Cronobacter sakazakii* in powdered infant formula (Pan *et al*., 2018). Furthermore, a larger number of diverse lateral flow immunoassays are commercially available (Singlepath®, Duopath®, RapidChek®) for the detection of food pathogens from pre-enriched samples (Dwivedi & Jaykus, 2011).

15

Although immunological based methods are fast and easy to perform, they need to be incorporated with today's technologies like optical and electrochemical transducers and wireless data transfer (Amerongen, Veen, Arends, & Koets, 2018). Another important future plan related to lateral flow immunoassay is using paper based materials instead of nitrocellulose because paper based materials can be used in a wide range of area (Amerongen *et al*., 2018).

1.3.2.2. Nucleic acid-based Methods

In this method, some specific RNA or DNA sequence in pathogen bacteria is detected. This is obtained by the hybridization of synthetic primers or probes which is complementary to the target gene found in pathogen bacteria (Law, Mutalib, Chan, & Lee, 2014). Since nucleic acid-based methods only detect the genes in target pathogen, the possibility of false positive results become relatively low. Simple polymerase chain reaction (PCR), nucleic acid sequence-based amplification (NASBA), multiplex polymerase chain reaction (mPCR), loop-mediated isothermal amplification (LAMP) and microarray technology are the recent examples of this method. Table 1.4 summarizes examples of these methods and foodborne detected.

Table 1.4 Detection of various foodborne pathogens found in food with nucleic acid-based methods (Law et al., 2014)

Detection method	Foodborne pathogens	Detection limit	Food matrix	Assay time	References
Multiplex PCR	Salmonella spp., Salmonella Enteritidis	10^3 CFU/mL	Artificially and naturally contaminated chicken carcasses, minas cheese and fresh pork sausages	24 h	Silva et al., 2011
	STEC O26, O103, O111, O145, sorbitol fermenting O157 non-sorbitol fermenting O157	5×10^4 CFU/mL in minced beef and sprouted seeds. 5×10^3 CFU/mL in raw-milk cheese	Artificially contaminated minced beef, sprouted seed (soy, alfafa and leek) and raw-milk cheese	24 h	Verstraete et al., 2012
	Escherichia coli O157:H7, Listeria monocytogenes Staphylococcus aureus, Yersinia enterocolitica, Salmonella	10^3 CFU/mL	Artificially contaminated pork	Not stated	Guan et al., 2013
Real-time PCR	Salmonella enterica	41.2 fg/PCR for Salmonella Typhimurium genomic DNA. 18.6 fg/PCR for Salmonella Enteritidis genomic DNA	Artificially contaminated chicken, liquid egg and peanut butter	10 h	Chen et al., 2010
	Listeria monocytogenes, Escherichia coli O157, Salmonella spp	<18 CFU/10 g	Artificially contaminated ground beef. Naturally contaminated beef, pork, turkey and chicken	24 h	Suo et al., 2010b
	Listeria monocytogenes, Escherichia coli O157:H7, Salmonella spp.	2×10^2 CFU/mL	Artificially contaminated ground pork	24 h	Kawasaki et al., 2010
	Salmonella spp., Listeria monocytogenes	5 CFU/25g	Artificially and naturally contaminated meat, fish, fruits, vegetables, dairy products, eggs, chocolate bar, omelet, lasagna, and various cooked dishes	<30 h	Ruiz-Rueda et al., 2011
	Staphylococcus aureus, Salmonella, Shigella	9.6 CFU/g for Staphylococcus aureus, 2.0 CFU/g for Salmonella and 6.8 CFU/g for Shigella	Fresh pork	<8h	Ma et al., 2014
NASBA	Escherichia coli	40 cells/mL	Drinking water	4 h	Min and Baeumner, 2002
	Salmonella Enteritidis	10^1 CFU/reaction	Artificially contaminated fresh meats, poultry, fish, ready-to-eat salads and bakery products	26 h	D'Souza and Jaykus, 2003
	Listeria monocytogenes	400 CFU/mL	Artificially contaminated cooked ham and smoked salmon slices	72 h	Nadal et al., 2007

(Continued)

Detection Method	Foodborne Pathogens	Detection Limit	Food Matrix	Assay Time	References
	Bacillus amyloliquefaciens, Bacillus cereus and Bacillus circulans	–	Artificially contaminated milk	Not stated	Gore et al., 2003
	Salmonella Enteritidis and Salmonella Typhimurium	<10 CFU/mL	–	<90 min	Mollasalehi and Yazdanparast, 2013
LAMP	Vibrio vulnificus	5.4 CFU/reaction for a virulent V. vulnificus strain in pure culture. 2.5×10^3 CFU/g for a virulent V. vulnificus strain in spiked raw oyster, no enrichment. 1 CFU/g for a virulent V. vulnificus strain in spiked raw oyster, after 6 h enrichment	Artificially contaminated raw oysters	8 h	Han et al., 2011
	Salmonella spp. and Shigella spp.	5 CFU/10 mL	Artificially contaminated milk	<20 h	Shao et al., 2011
	Vibrio parahaemolyticus	10 CFU/reaction	Naturally contaminated seafood samples: fish, shrimp and mussel	16 h	Wang et al., 2013a
	STEC O26, O45, O103, O111, O121, O145, and O157	1–20 cells/reaction in pure culture and 10^5–10^6 CFU/25 g in produce	Artificially contaminated lettuce, spinach and sprouts	Not stated	Wang et al., 2014
Oligonucleotide DNA microarray	Escherichia coli O157:H7, Salmonella enterica, Listeria monocytogenes and Campylobacter jejuni	1×10^{-4} ng for each genomic DNA	Naturally contaminated fresh meat samples: chicken, beef, pork and turkey	Not stated	Suo et al., 2010a
	Listeria monocytogenes	8 logCFU/mL	Artificially contaminated milk	Not stated	Bang et al., 2013
	Escherichia coli, Shigella spp., Salmonella spp., Proteus sp., Campylobacter jejuni, Listeria monocytogenes, Enterococcus faecalis, Yersinia enterocolitica, Vibrio parahaemolyticus, Vibrio fluvialis, β-hemolytic Streptococcus, Staphylococcus aureus	10 CFU/mL of pure culture	Artificially and naturally contaminated pork, chicken, fish and milk	Not stated	Huang et al., 2014

1.3.2.3. Biosensors

Biosensors are a type of analytical device and they are composed of two fundamental components: a bioreceptor and a transducer. The bioreceptor can be a biomimic like imprinted polymers and synthetic catalysts; a biological material such as nucleic acids, enzymes, antibodies; biologically derived material such as aptamers and recombinant antibodies. The transducers, on the other hand, converts biological interactions into a detectable elements that can be optical, electrical, electrochemical, thermometric, piezoelectric, amperometric and recently mass-based (Arora, Sindhu, Dilbaghi, & Chaudhury, 2011) (Law *et al*., 2014)

The most advantageous feature of biosensors compared to nucleic acid based methods and immunological methods is that pre-enrichment is not needed before the detection of pathogens (Singh, Poshtiban, & Evoy, 2013). Another great aspects of biosensors that they can give real-time results and detect multiple pathogens for both field and *in vitro* analysis (Zhao, Lin, Wang, & Oh, 2014).

Nowadays, biosensors have been used and improved in order to identify important food pathogens such as *E.coli* O157:H7, *Staphylococcus aureus*, *Salmonella*, and *Listeria monocytogenes* and their microbial toxins (Zhao *et al*., 2014). Table1.5 shows the different type of biosensor based foodborne detection.

Table 1.5 Different types of biosensor for the detection of food pathogens (Zhao et al., 2014)

Mode of detection	Analyte	Limit of detection	Assay time
Optical biosensor	*Escherichia coli* O157:H7	5×10^5 cells/ml	45 min
	Escherichia coli O157:H7, *Yersinia enterocolitica*, *Salmonella* Typhimurium, and *Listeria monocytogenes*	10^4 CFU/ml for all bacterial species	
	Escherichia coli O157:H7	10^6 cells/ml	
	Salmonella Typhimurium	10^5 CFU/ml	12 h
Surface plasmon resonance biosensor	*Escherichia coli* O157:H7	3×10^5 CFU/ml	5 to 7 min
	Escherichia coli O157:H7	10^2 CFU/ml	2 min
	Escherichia coli O157:H7	8.7×10^6 CFU/ml	35 min
	Salmonella Typhimurium	1×10^6 CFU/ml	
	Salmonella enteritidis and *Escherichia coli*	25 CFU/ml for *Escherichia coli* and 23 CFU/ml for *Salmonella*	<1 h
Piezoelectric biosensors	*Escherichia coli* O157:H7		
	Bacillus anthracis	300 spores/ml	
	Escherichia coli O157:H7, staphylococcal enterotoxin B		
Immunosensors	*Escherichia coli* O157:H7	4.12×10^2 CFU/ml	<45 min
	Salmonella Typhi	10^5 cells/ml	90 min
	Salmonella	2.43 log CFU/ml	4 h
Electrochemical biosensors	*Escherichia coli* O157:H7	10^2 CFU/ml	
	Salmonella Typhi		1 h 15 min
	Bacillus cereus	35−88 CFU/ml	6 min

1.3.2.3.1. Lateral Flow Biosensors

Lateral Flow Assays or Lateral flow immunochromatographic tests are a type of paper-based biosensors. First commercially sold LFA was urine-based pregnancy test which was created by Unipath in 1984 (Mak, Beni, & Turner, 2016).

The main advantageous of Lateral Flow Biosensors (LFBs) are high sensivity, reliable selectivity, quickness, robustness, easy handling, simplicity and low-cost (X. Zhang, Xu, Zhou, Liu, & Gao, 2014). However, there are also some disadvantages related with LFBs. The first one is about their qualitative but not quantitative results which are identified with naked eye. On the other hand, results can be semiquantitative via some reading devices. Another drawback is about liquid sample which must have enough velocity to travel through porous of nitrocellulose paper. Sometimes

pretreatment or predilution of sample could be needed since there is a possibility that these porous can be blocked by different matrix compounds (Quesada-González & Merkoçi, 2015).

LFBs are able to detect numerous types of biocompounds such as nucleic acids, proteins, cells. For instance, Alere Determine HIV-1/2 Ag/Ab ComboIn, rapid LFIA kit for the detection of p24 antigen as well as antibodies to HIV-1 and HIV-2, is now permitted by FDA (Jaiswal, 2018). In addition, LFBs can be used in the simultaneous detection of pollutants such as carbofuran and triazophos (Guo, Liu, Gui, & Zhu, 2009) and uranium (Quesada-González, Jairo, Blake, Blake, & Merkoçi, 2018) ; carcinogenic toxin like aflatoxin B1 in crops (Y. Zhao *et al*., 2016) and zearalenone (Chen, Fu, Xie, Wang, & Tang, 2019) ; toxic heavy metals like mercury (Y. Zhang *et al*., 2012) and cadmium (S. Song, Zou, Zhu, Liu, & Kuang, 2018).

Lateral Flow Assays (LFAs) are designed in the strip form which is easy to use. Their width generally between 4 and 6 mm and a length no more than 6–7 cm. LFAs are composed of 4 basic components as illustrated in Figure 1.9: a sample pad, a conjugate pad, a detection pad and an absorption pad. Sample is loaded on cellulose or cross-linked silica sample pad and transmitted to a conjugate pad which is preloaded with bio-recognition molecules such as receptors or labelled analytes. Detection pad or assay membrane is the largest part of the LFAs and it influences the sensitivity of assay (Dong, Zhao, Wang, Zhang, & Liu, 2017). Test line (TL) and Control line (CL) are located on this nitrocellulose sheet. Finally, waste is collected in the adsorption pad which is also made of cellulose
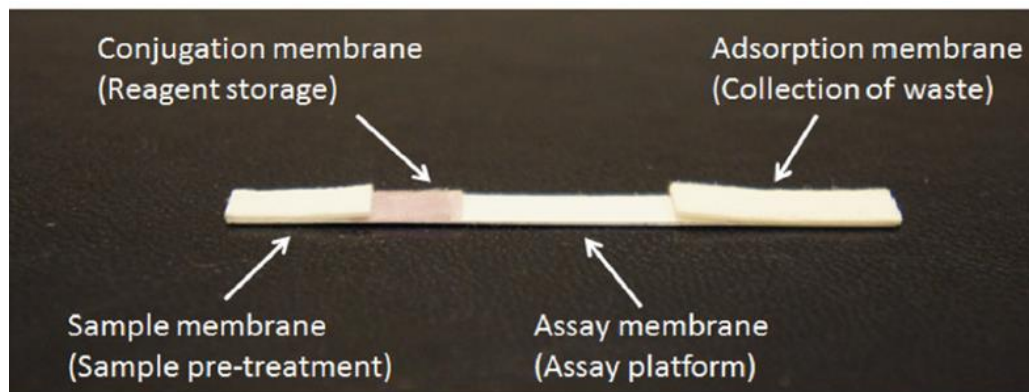
Figure 1.9 Simple design of the lateral-flow test and its components (Mak et al., 2016)

In standard Lateral Flow Assay, analyte and bioreceptor (transducer) are linked to each other in the conjugate pad and flow along detection pad and captured in Test Line. On the other hand, there is also a competitive model which analyte and transducer compete each other to be captured by TL. As a result, there exists an inverse proportion between concentration of analyte and response in TL (Quesada-González & Merkoçi, 2015). Figure 1.10 represents standard and competitive diagrams of LFAs.
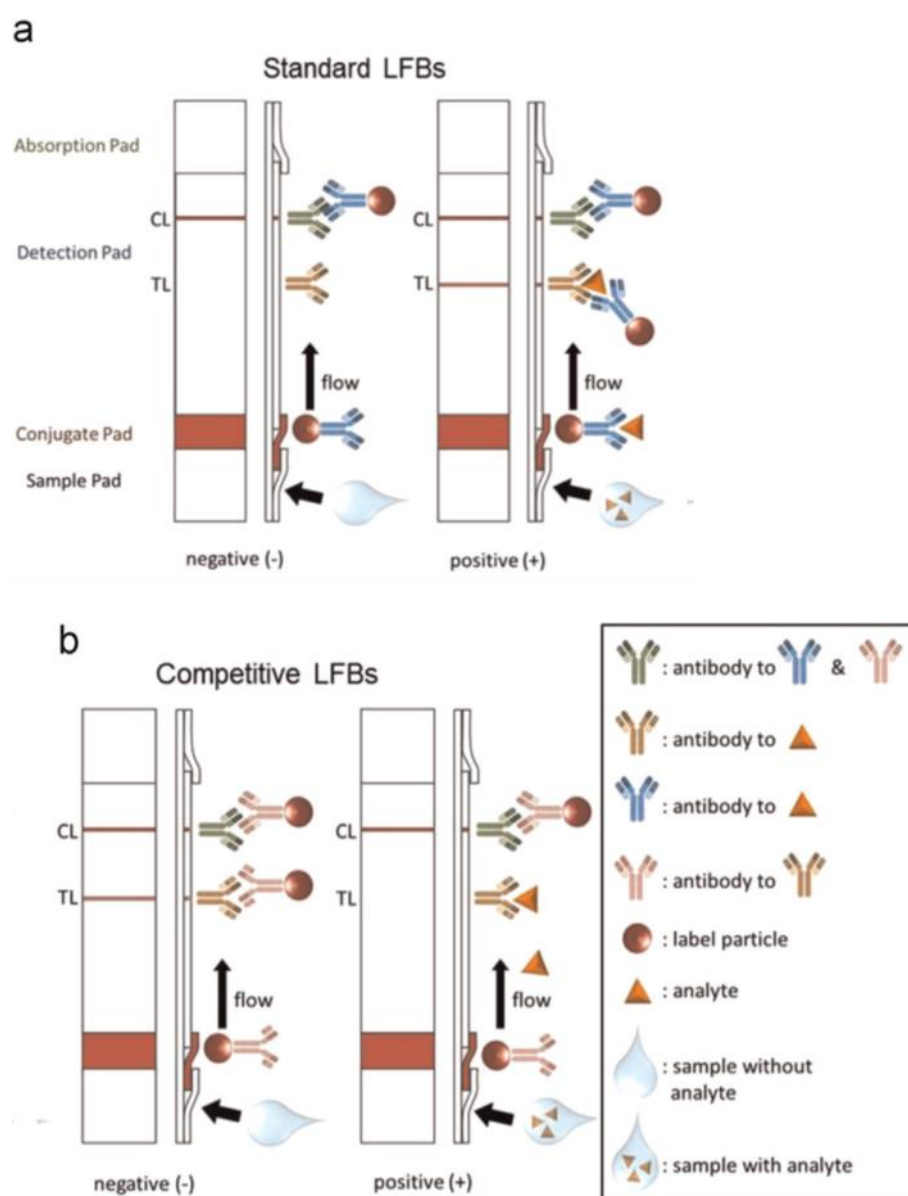
Figure 1.10 Schematic representation of LFAs (a) standard LFBs (b) competitive LFBs (Quesada-González & Merkoçi, 2015)

The most widely used nanomaterial for lateral flow tests in the literature is gold nanoparticles (AuNPs). Because AuNPs are easy to produce, stable for a long time, biocompatible and their sharp red color easily identified even via naked eye (Quesada-González & Merkoçi, 2015). Another visual labelling system for LFAs is Carbon

nanoparticles (CNPs). It has low-cost compared to gold and polymer-based nanoparticles. In addition, its strong black color provides an easy and quick detection. Nevertheless, because of its hydrophobic surface and reduced colloidal stability, CNPs can not efficiently conjugate with biomolecules (Mak *et al*., 2016). Another nanomaterial used as a label is selenium nanoparticle. Although its intensity is low compared to gold nanoparticles, Wang *et al*. (2014) advocates the cost effectiveness of selenium material in comparison to AuNPs. There are also other alternatives to AuNPs such as silver nanoparticles and platinum nanoparticles.

Mesoporous silica materials are another important candidate in sensor technology because they are non-invasive and biocompatible. Moreover, they consist of highly ordered pores with large load capacity and their pore size can be easily adjusted. All of these features make mesoporous silica nanoparticles good carrier vehicles for various biotechnological applications especially for the drug delivery (Y. Zhang *et al*., 2012). They are in different poor sizes between 2 to 10 nm and MCM-41,MCM-48 and SBA-15 are the best known porous silica nanoparticles (P. Yang, Gai, & Lin, 2012). After It was noticed that pores of mesoporous-silica-nanoparticles show controlled release depending on the changes in pH, redox potential, and light, It has been targeted in the use of delivering of some bio-molecules like a bio-gates (Climent *et al*., 2010). Recently, colored SiNPs was started to be used as a nanomarker alternative to other labelling methods and clenbuterol was detected successfully (Zhu, Zhao, & Dou, 2018).

1.4. Aim of the Study

In this thesis, *E. coli* O157:H7 will be detected with LFA by the application of mesoporous silica nanoparticles (MSP-SiNPs). MSP-SiNPs, loaded with 3,3,5,5-Tetramethylbenzidine (TMB), were covered with oligonucleotide probes, which is also complementary sequences to *eaeA* gene found in *E.coli* O157:H7. The complementary target sequence oligonucleotides will remove the probes from the SiNP surface and release the TMB. To obtain an efficient colorimetric reaction, optimization assays were conducted. As a result of these studies, the SiNP-based LFA system to be developed will be expected to selectively and sensitively detect E. coli O157: H7 and other bacteria with the target amplicon.

CHAPTER 2

MATERIALS AND METHODS

2.1. Materials

2.1.1. Chemicals

All of the chemicals that were used in this study were purchased from Merck, AppliChem, Sigma-Aldrich, Thermo Fisher Scientific and NanoBiz companies.

2.1.2. Bacterial Strains

In this study, two different *Escherichia coli* serotypes *Escherichia coli* O157:H7 (ATCC 700728) and *Escherichia coli* O6 (ATCC 25922), *Pseudomonas Aeruginosa* (ATCC 27853) and *Salmonella enterica* Serovar Enteritidis (ATCC 13076) were used for genomic DNA purifications and polymerase chain reactions. All these strains were purchased from American Type Culture Collections (USA).

2.1.3. Buffers and Solutions

All solutions were formed with dH_2O. Contents and compositions of solutions of buffers were shown in Appendix A.

2.1.4. Oligonucleotides

Oligonucleotides used in this study were composed of probes, targets, control targets and primers. Their sequences are listed in Appendix A. Primers were used for PCR amplification of *eaeA* gene found in *E.coli* O157:H7. Probes were used to cap nanoparticles while targets were designed to be complementary to these probes. Control targets were not comprised of any complementary sequence to probes.

Stock solutions of primers were adjusted as 100 μM with MilliQ water as stated in company's description and kept at -20 °C for long term usage. 10 μM primer working solutions were arranged from the stock solution for PCR reaction.

Stock solutions of probes, targets and control targets were prepared as 1000 μM using MilliQ water based on the guidelines provided by the manufacturer and kept at -20 °C for long term. For LFA experiments, 100 μM working solutions of all were prepared from stock solutions.

All designed oligonucleotides were obtained from Oligomer Biotechnology A.Ş.

2.2. Methods

2.2.1. Target Preparation

2.2.1.1. Growth conditions of *Escherichia Coli*

E.coli cultures were grown overnight at 37°C in Luria-Bertani (LB) broth with shaking at 120 rpm. *Salmonella* cultures were incubated at 37°C for 18 hours in Tryptic soy broth (TSB) by incubating on rotary shaker (100 rpm) . The inoculated cultures of *P. aeruginosa* were grown in LB broth for 18 hours at 37°C with shaking at 200 rpm. Compositions of mediums were given in Appendix A.

2.2.1.2. Isolation of *Escherichia Coli* genomic DNA

Genomic DNA isolation was accomplished using NANObiz DNA4U Bacterial Genomic DNA Isolation kit according to the manufacturer's guides with some modifications. Furthermore, manuel DNA isolation was also carried out. Then, phenol extraction and ethanol precipitation of DNA was done to purify sample

2.2.1.3. Polymerase Chain Reaction of *eaeA* gene

First of all, gradient PCR was done to demonstrate optimal annealing temperature. Employing the gradient function of the thermal cycler, a gradient of 50 to 60°C (50.7,51.9, 53.7, 56.1, 58.0, 59.2) was arranged. And then, conventional PCR was done to obtain *eaeA* gene. Components, concentrations and temperature conditions of gradient PCR for 103 bp *eaeA* gene (*E.coli* O157:H7) were shown in Table 2.1, Table 2.2 and Table 2.3, respectively.

Table 2.1 The optimized PCR condition in 20 µL for 103bp for eaaA gene (Target Amplicon)

PCR components	Volume 1X (µL)	Final Concentration
dH$_2$O	12.7	-
10X buffer	2	0.8X
25 mM MgCl2	1.4	1.4 mM
10 µM Forward Primer	0.6	0.24 µM
10 µM Reverse Primer	0.6	0.24 µM
10 mM dNTP	0.5	0.2 mM
5 U/µL Taq Pol	0.2	0.08 U
DNA template (20ng/µL)	2	-
Total volume	20	

Table 2.2 Gradient PCR conditions for 103bp for eaaA gene (Target Amplicon)

Step		Temperature (°C)	Time
Initial Denaturation		95	5 minutes
35 Cycles	Denaturation	94	30 seconds
	Annealing	50-60	30 seconds
	Extension	72	30 seconds
Final Extension		72	3 minutes

30

Table 2.3 Optimized temperatures of PCR for 103bp for eaaA gene (Target Amplicon)

Step		Temperature (°C)	Time
Initial Denaturation		95	5 minutes
35 Cycles	Denaturation	94	30 seconds
	Annealing	50.7	30 seconds
	Extension	72	30 seconds
Final Extension		72	3 minutes

2.2.1.4. Agarose Gel Electrophoresis

Agarose (750 mg) was dissolved in Tris/Acetate EDTA buffer (50 mL; TAE) by heating in a microwave until boiling. Ethidium bromide was added (0.05 µg/mL) to this gel solution after cooling. Gels (1.5 %) were poured a 10 x 20 cm gel tank, bubble formation was carefully avoided and then the comb was placed into the tray and the gel solidified. Gel electrophoresis was carried out with 1X TBE buffer. Amplicons mixed with 6X loading dye (Thermo Scientific, USA) and DNA ladders, previously mixed with 6X loading dye, were loaded into the gel's wells and they was run at 75V for 1h. Later, gels were imaged by UV acquisition system. This technique was used for the analysis of *eaeA* gene which is specific to *Escherichia coli* O157:H7.

2.2.1.5. Synthetic Target Preparation

Synthetic targets used as a 1000 μM stock were preperad according to the company's guide were dissolved in DNase/RNase free dH₂O. 100 μM working solution was made up from 1000 μM stock target. Then, they were employed for assay studies and the determination of LOD (limit of detection) values. Control target was also arranged in a similar way.

2.2.2. Preparation of Silica Nanoparticles for Colorimetric Assay

2.2.2.1. Entrapping of TMB into SiNPs

In this part, 3,3′,5,5′-Tetramethylbenzidine (Sigma-Aldrich, Germany), a peroxidase sensitive dye, was loaded into SiNPs. First, 2.5 mg of SiNPs were suspended in 495 μL of 1X PBS. Then, SiNPs solution was sonicated for 10 minutes. 5 μL of 0.5 M TMB solution was added. TMB-SiNPs were vortexed and afterwards they incubated overnight in 2D shaker for 24 hours at 37.5 °C with 50 rpm (Heidolph DuoMax 1030). For this experiment, 1 M TMB stock solution and 0.5 M and 0.2 M working solutions were prepared.

2.2.2.2. Silanization of TMB loaded SiNPs

The purpose of this part is to functionalize the external surface of SiNPs with aminopropyltriethoxysilane(APTS). Aminopropyl groups will interact with negatively charged oligonucleotides because they have partially positive charge at neutral pH in water (Climent *et al.*, 2010). After 24 hours incubation of SiNPs with TMB, TMB-SiNPs were centrifugated for 5 minutes at 8°C with 6000 rpm (MPV-65R). Supernatant was discarded and pellet was washed with 500 μL of 1X PBS. This step was repeated once more to get rid of excess TMB. After final centrifugation step, supernatant was discarded and then 475 μL of 1X PBS and 25 μL of 3-Aminopropyl-trimethoxysilane (APS) was added for silanization. APS-SiNPs were incubated for 3 hours at 37.5 °C with 50 rpm (Heidolph DuoMax 1030).

2.2.2.3. Capping SiNPs with oligonucleotide probe

After silanization process, tubes were centrifugated for 5 minutes at 8 °C with 6000 rpm (MPV-65R), supernatant was eliminated and pellet was solved in 500 μL 1X PBS. This step was repeated for three times to eliminate the excess silane molecules from surface of nanoparticles efficiently. Then, silanized SiNPs were separated into 5 centrifugation tubes, immediately after last addition of 500 μL 1X PBS. These five tubes were again centrifugated for 5 minutes at 8 °C with 6000 rpm and supernatant was discarded. Later on, they were placed in an incubater (C. Gerhardt, Germany) for 20 minutes at 37.5 °C to evaporate excess supernatant. 10 μL of 100 μM oligonucleotide probe and 10 μL of 1X PBS were added onto pellet. For NULL SiNPs, on the other hand, milliQ water was used instead of oligonucleotide solution. These five mixtures were incubated for 1 hour at 37.5 °C shaking with 50 rpm in shaker found in incubator (C. Gerhardt). At the end of incubation, lids of tubes were opened and dried overnight at room temperature. Therefore, amino-functionalized surface could accept negatively charged phosphate backbone of oligonucleotide probes via electrostatic interaction.

2.2.3. Preparation of Lateral Flow Assay Platform

2.2.3.1. Schematic illustration of the lateral flow assay

Different types of arrangements are maintained in LFA system. Generally, strips used for LFA consist of four essential components which are sample pad, conjugate pad, nitrocellulose membrane and adsorbent pad. In this study, LFA platforms consisted of three parts except conjugate pad and they had 3 mm width. Functional SiNPs were placed onto LFA platform 6 mm away from sample pad while HRP was placed onto LFA platform 3 mm below SiNPs. The schematic representation of LFA was shown in Figure 2.1.
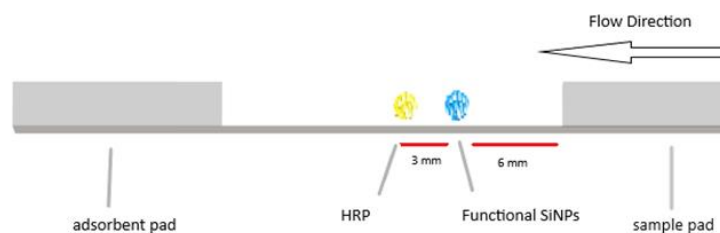
Figure 2.1 Schematic representation of Lateral Flow Assay Platform

2.2.3.2. Treatment of Samples on LFA

Sample loaded on LFA system was composed of either H_2O_2 and synthetic targets or H and amplicons. H was prepared from 30 % (weight / volume) stock solution and final concentration was arranged to 1.5 % (weight / volume). Synthetic targets and amplicons were incubated 95 °C for 5 minutes in thermal cycler (Bio-Rad) and they were immediately carried into icebox. In this way, formation of double stranded DNA could be prevented and yield of single stranded DNA could be improved. Because, ssDNA were obligatory for this experiment in order to provide effective matching of target with probe which cover nanoparticle. Before TMB loaded nanoparticles were placed on strips, they were suspended with 50 µL 1X PBS and centrifugated for 5 minutes at 8 °C with 6000 rpm. After centrifugation was done, supernatant was discarded and 10 µL 1X PBS was added onto nanoparticles. Then, 1 µL mixture of 1X PBS and nanoparticle was placed onto strip. 1 µL HRP was placed subsequently below the nanoparticle after a 10 minute interval. For each strip, 26 µL of H_2O_2 (1.5 %) and 14 µL of targets were mixed on ice and travel through the sample pad. After 5 minutes, alteration of color was monitored in the circular area of SiNPs on LFA platform

2.2.4. Quantification of Color on LFA

The image analysis system for the lateral flow strip was composed of Stereomicroscope (1X) (Nikon, SMZ800) and imageJ software. First, images of each strip were acquired by Stereomicroscope (1X) (Nikon, SMZ800). Then, images were analyzed by the help of ImageJ software. First, picture of strip was converted to gray scale image. Then, imageJ converted gray values to uncalibrated density values. Notably, the conversion could only be carried out on 8-bit images. The intensity of the test, control and negative area was measured by lanes via plotting graph. Calibrated value (in our case, signal intensity) can be obtained by the below formula from the graph. This represents the average gray value within the selected part. In other words, total gray values of all the pixels in the selected part divided by the number of pixels. (Ferreira & Rasband, 2012)

$$SI = \log_{10}(255/\text{pixel value})$$

2.2.5. Statistical Analysis

IBM SPSS Statistics 25 was employed for statistical analysis of SI: mean, standard deviation and ANOVA. For all data obtained in this study, One-way ANOVA and Two-way ANOVA at 95% Confidence Interval and Tukey HSD tests were performed.

CHAPTER 3

RESULTS AND DISCUSSION

3.1. General Principles of Experiment

In this study, synthetic target for *eaeA* gene from *E.coli* 0157:H7 was used. SiNPs were capped with probes which hybridize with this synthetic target. SiNPs were loaded with TMB, and when probe and target hybridized, TMB was released, H_2O_2/HRP oxidized TMB and blue color formation was occurred. Colorimetric reaction and lateral flow assay parameters were optimized. Using optimal conditions, it was excepted to observe blue color with naked eye. Thus, quick *E.coli* detection was possible.

3.1.1. Optimization Studies

3.1.1.1. Optimization of Colorimetric Reaction Parameters

In this part, optimum conditions for Lateral Flow Assay Platform was evaluated. First, different concentrations of components found in TMB-H_2O_2-HRP system were compared. Then, the duration and temperature of important steps, features of the nitrocellulose membrane were studied. Finally, after proper conditions of LFA for the synthetic target were optimized, the PCR product of the *eaeA* gene was introduced to the system to verified the LoD.

3.1.1.1.1. Effect of Different Concentrations of Hydrogen Peroxide

In this part of study, effect of H_2O_2 with different concentrations on LFA was evaluated. Both TMB and H_2O_2 concentrations influence the reaction kinetics because initially HRP interacts with H_2O_2 to constitute an enzyme-oxygen free radical and afterwards the reaction occurs between the free radical and TMB (Gao, Wu, & Gao, 2011). For this purpose, NULL SiNPs which are not capped with oligonucleotide probes, were used. Since hydrogen peroxide (H_2O_2) manages the rate of the enzymatic conversion of TMB to blue color, it was accepted as a limiting factor for this reaction. Hence, H_2O_2 with 1 %, 1.5 %, 2.5 % and 3.5 % (w/v) were examined in optimization assays to obtain more accurate results.

As a result of one-way ANOVA, there was a nonsignificant main effect of H_2O_2 concentration on signal intensity, F (3, 8) = 2,335, p = ,150. Which means that there were no meaningful differences between the concentration of H_2O_2 (1 %, 1.5 %, 2.5 %, 3.5 %). Thus, 1.5 % (w/v) H_2O_2 was chosen for this experiment because; for low (1 %) H_2O_2 concentration, H_2O_2 was not able to contact with HRP effectively and production of blue color was low. On the other hand, for high (3.5 %) H_2O_2 concentration, HRP is very close with H_2O_2/TMB and possibility of background signal occurrence was increased (Fung, Chan, & Renneberg, 2009).
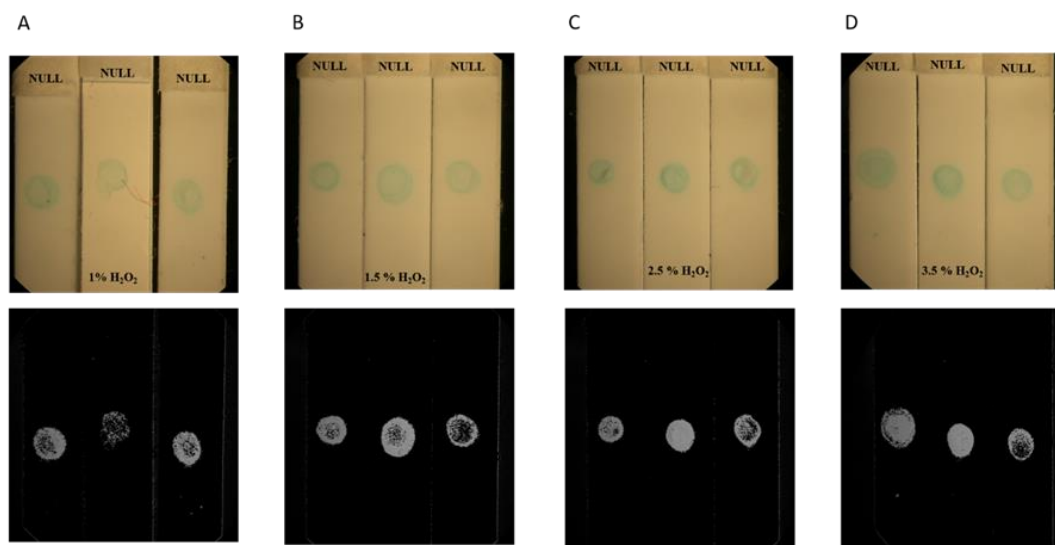
Figure 3.1 LFA with Colorimetric reaction results for four different concentrations (1 %, 1.5 %, 2.5 %, 3.5 %) of Hydrogen Peroxide. SiNPs were entrapped with 5mM of TMB (1 mg/mL of HRP and 37 ℃) and silanized but not capped with probes -so called 'NULL' . Signal intensities (SI) of the results were measured by ImageJ program and converted into 8 bit grayscale image which was found below the original photos. A) 1 % (w/v) H_2O_2 was applied. B) 1.5 % H_2O_2 was loaded. C) 2.5 % H_2O_2 was added D) 3.5 % H_2O_2 was applied.

Table 3.1 Descriptive statistics of given data set for different H_2O_2 concentrations (Dependent Variable: SI)

H_2O_2.concentration	Mean	Std. Deviation	N
1 % H_2O_2	31322,6937	14279,08367	3
1.5 % H_2O_2	47590,1140	14068,15642	3
2.5 % H_2O_2	49050,2953	12170,09094	3
3.5 % H_2O_2	59232,0767	11619,32757	3
Total	46798,7949	15282,86390	12
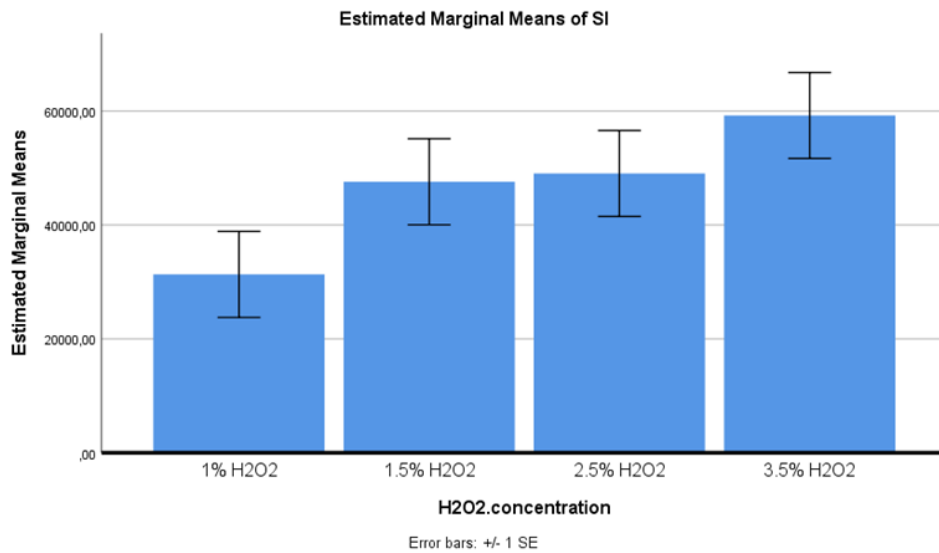
Figure 3.2 Signal Intensity (SI) for various H_2O_2 concentrations 1%,1.5%,2.5%,3.5% (w/v) on LFA with NULL (nanoparticles were not capped with oligonucleotide probes) SiNPs. A one-way ANOVA was conducted that examined the effect of H_2O_2 on SI. There were no significant differences between different H_2O_2 concentrations on SI, $F (3, 8) = 2,335, p = ,150$.

Table 3.2 Tests of Between-Subjects Effects (Dependent Variable: SI)

Source	Type III Sum of Squares	df	Mean Square	F	Sig.	Partial Eta Squared
H_2O_2 concentration	1199374934,979	3	399791644,993	2,335	,150[ns]	,467

R Squared = ,467 (Adjusted R Squared = ,267)

3.1.1.1.2. Effect of Different Concentrations of 3,3′,5,5′-Tetramethylbenzidine (TMB)

TMB represents the peroxidase activity in hydrogen peroxidase with the help of HRP, and it is called chromogenic substrates (Bahadır & Sezgintürk, 2016). Depending on the length of this reaction; blue, green and yellow colors can be seen since TMB is oxidized to a cation free radical (blue) and diimine (yellow) (Lathwal & Sikes, 2016). In this part, effect of different TMB concentrations (1mM, 5 mM and 10mM) were observed to obtain higher signal intensity with maximum specificity. First of all, two-way ANOVA was conducted to understand whether independent variables (TMB concentrations and Target Types) had an effect on Signal Intensity (SI). According to significance values of independent variables (two-way ANOVA, $p < 0.001$), there was a significant effect of both on SI as can be seen in table 2. Then, TUKEY HSD showed that SI was significantly different for 1mM and 5mM, $M_{diff} = -14006.12$, 95% CI [-26303.76, -1708.50], $p = .024$ and for 1mM and 10Mm, $M_{diff} = -31738.39$, 95% CI [-44036.02, -19440.75], $p = .000$, and significantly different for 5mM and 10Mm, $M_{diff} = -17732.26$, 95% CI [-30029.90, --5434.63], $p = .005$. So, it can be said that increased TMB concentration gave increased intensity as it was expected. However, although SiNPs loaded with 10mM of TMB gave high amount of SI compared to 5mM of TMB, its specificity was not as reliable as 5mM. Because, high amount of SI was also detected on LFA result with control target. Moreover, another important point related with this result was the background signal increasing with the TMB concentration.While, there was a negligible background signal with 1mM loaded SiNPs, 10 mM loaded SiNPs gave high signal intensity in control strip. This was probably because of the interaction between excess TMB found in the surface of SiNPs and the control target. Normally, control target could not hybridize with the probes which cap pores of SiNPs. However, this interaction may cause the accumulation of both TMB and control target on the surface and damage the electrostatic interaction between aminated parts

and probes. Therefore, SiNPs might be partially capped with probes and TMB released to outside.
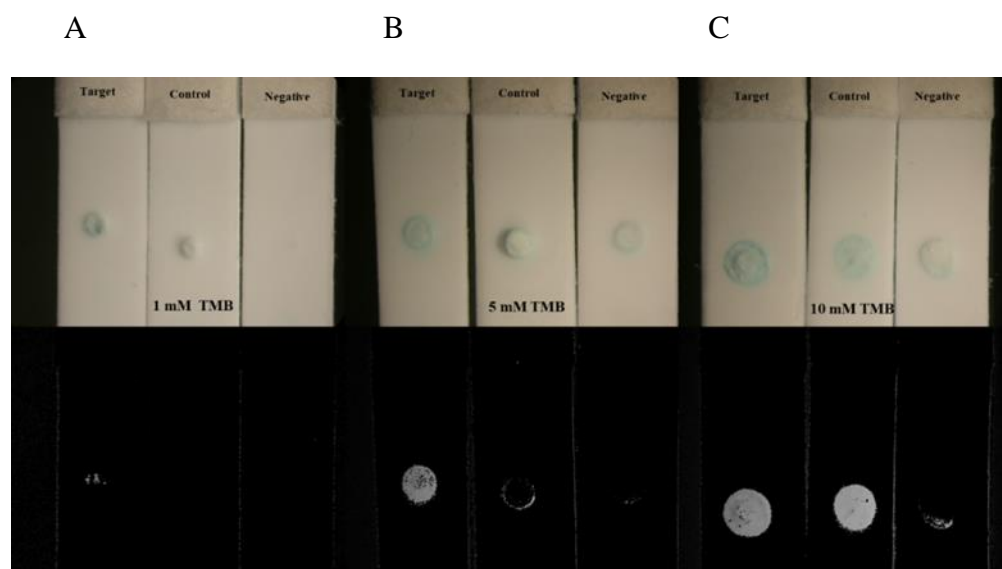
Figure 3.3 Outcome of three different concentrations of TMB on LFA. SiNPs were loaded with 1mM, 5mM and 10 mM of TMB respectively. SiNPs with probe capped pores were placed on LFA setup. (1.5% H₂O₂, 1 mg/mL of HRP and RT) Target (composed of complementary sequence), Control (including uncomplementary sequence) were sent with 1.5% H₂O₂ to LFAs. Instead of nucleic acids, water and 1.5% H₂O₂ was applied as negative. A) SiNPs with 1mM final concentration of TMB B) SiNPs with 5mM final concentration of TMB C) 10 mM final concentratıon of TMB loaded SiNPs

Table 3.3 Descriptive statistics of given data set for different TMB concentrations (Dependent Variable: SI)

TMB concentration	Target type	M	SD	N
1mM	complementary	37483,4953	6151,06256	3
	uncomplementary	5476,5753	4825,13791	3
	negative	,0000	,00000	3
	Total	1. 14320,023 6	17964,14234	9
5mM	complementary	75722,5487	4639,67915	3
	uncomplementary	7622,9937	7610,95512	3
	negative	1632,9010	1108,28055	3
	Total	28326,1478	35923,65096	9
10mM	complementary	84565,3070	5012,31396	3
	uncomplementary	50528,3637	27722,95256	3
	negative	3081,5617	2201,71886	3
	Total	46058,4108	38154,91318	9
Total	complementary	65923,7837	22153,12487	9
	uncomplementary	21209,3109	26397,63934	9
	negative	1571,4876	1817,02742	9
	Total	29568,1940	33458,31030	27
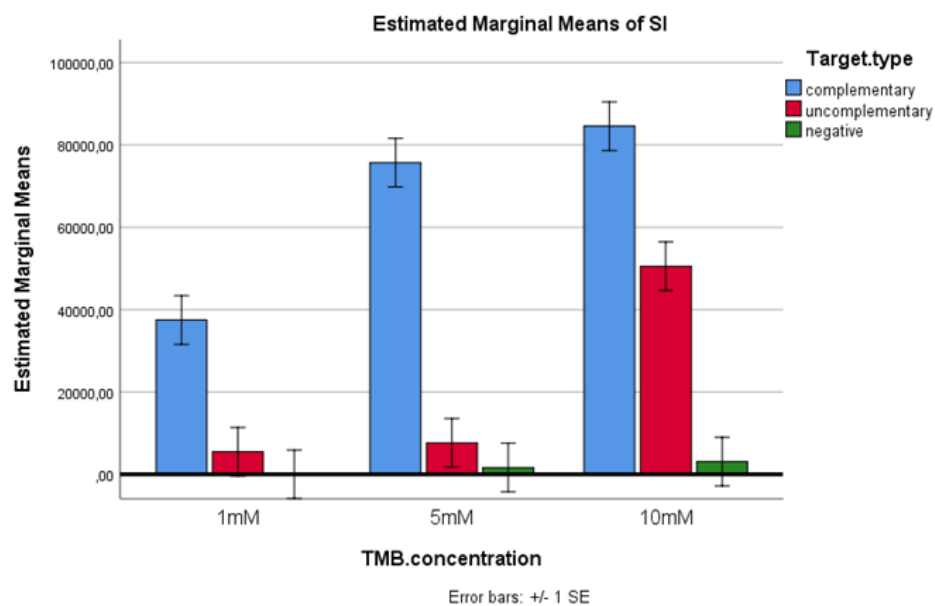
Figure 3.4 Signal Intensity (SI) for different TMB concentrations 1mM, 5 mM and 10mM on LFA with probe capped SiNPs. A two-way ANOVA was conducted that examined the effect of TMB concentrations and target types on SI. There was a statistically significant interaction between the effects of TMB concentrations and target types on SI, $F_{(4, 18)} = 7.400$, $p = .001$.

Table 3.4 Tests of Between-Subjects Effects (Dependent Variable: SI)

Source	Type III Sum of Squares	df	Mean Square	F	Sig.	Partial Eta Squared
TMB conce	4553789670,89	2	2276894835,446	21,792	,000**	,708
Target type	19578738587,51	2	9789369293,757	93,695	,000**	,912
TMB conc. * Target type	3092729417,93	4	773182354,48	7,400	,001**	,622

R Squared = ,935 (Adjusted R Squared = ,907)

3.1.1.1.3. Effect of Different Concentrations of Horseradish Peroxidase (HRP)

Assay sensitivity and the intensity of test line colors can be easily managed by the addition of HRP thanks to the catalytic properties of enzymes (Eltzov *et al*, 2015). Although, Horseradish peroxidase (HRP) is one of the most commonly used enzymes for colorimetric assays, it is easily influenced by acidity, temperature, and some sort of inhibitors (Zhang *et al*., 2019). So, determining proper concentration and working conditions of HRP is very crucial for the next steps. In this part of optimization, different concentrations of HRP (0.25 mg/mL, 0.50 mg/mL, 0.75 mg/mL and 1 mg/mL) were used in experiments. It was concluded that an interaction between HRP concentration and target type could not be demonstrated, $F_{(5,25)} = 1.5$, $p = .230$. However, a significant main effect was obtained for HRP concentration, $F_{(3,25)} = 15.075$, $p < .001$. In this case, there was a meaningful difference found between different HRP concentrations. Especially, 1 mg/mL HRP concentration had

significantly higher SI (M=34313.34) than 0.25 mg/mL HRP concentration (M=10359,79). A significant main effect was also obtained for target type, $F_{(2,25)}$ = 58.75, indicating that complementary target had significantly higher SI (M = 40748.91) than uncomplimentary (M = 10049.16) and negative (M = 3733.91). Considering the experimental results, 1mg/mL HRP concentration was chosen for the rest of the study.
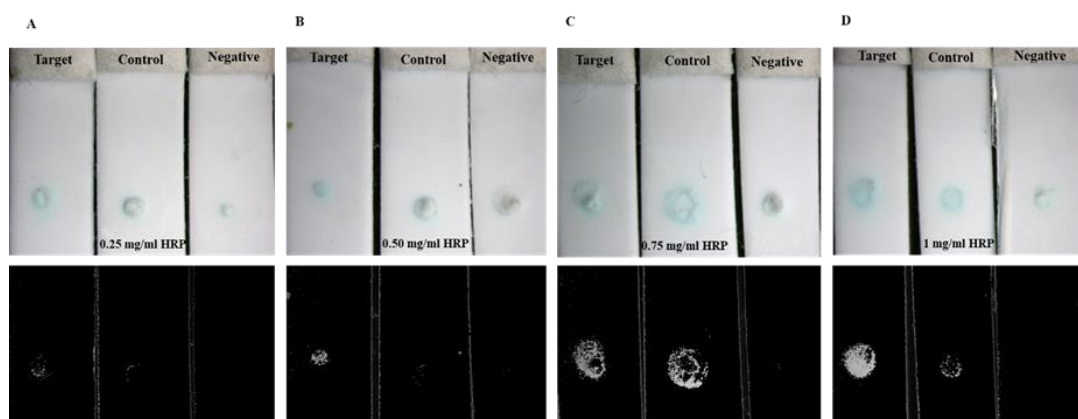
Figure 3.5 Colorimetric results on LFA with four different concentrations of HRP. SiNPs were loaded with 5mM of TMB. SiNPs with probe capped pores were placed on LFA platforms. (RT) Target (formed from complementary sequence), Control (originated from uncomplimentary sequence) were applied with 1.5% H_2O_2 to LFAs. Instead of nucleic acids, water and 1.5% H_2O_2 was applied as negative. A) The effect of 0.25 mg/mL of HRP on LFA B) The effect of 0.5 mg/mL of HRP C) The response of LFAs for 0.75 mg/mL of HRP D) The response of LFAs for 1 mg/mL of HRP

Table 3.5 Descriptive statistics of given data set for different HRP concentrations (Dependent Variable: SI)

HRP concentration	Target type	Mean	Std. Deviation	N
0.25 mg/mL	complementary	23539,3040	9320,82262	3
	uncomplementary	7432,0233	5922,84995	3
	negative	108,0307	109,82996	3
	Total	10359,7860	11758,24087	9
0.50 mg/mL	complementary	39441,4977	12030,46027	3
	uncomplementary	4125,4530	6930,91273	3
	negative	70,5357	83,68548	3
	Total	14545,8288	19997,78448	9
0.75 mg/mL	complementary	34820,5950	3895,85991	3
	uncomplementary	5512,2757	2501,94785	3
	negative	174,2903	116,77276	3
	Total	13502,3870	16320,00423	9
1 mg/mL	complementary	65194,2310	7798,61478	3
	uncomplementary	26788,8753	16256,46526	3
	negative	10956,9030	18917,88596	3
	Total	34313,3364	27461,94041	9
Total	complementary	40748,9069	17599,08872	12
	uncomplementary	10964,6568	12524,39764	12
	negative	2827,4399	9439,79710	12
	Total	18180,3346	21164,72440	36
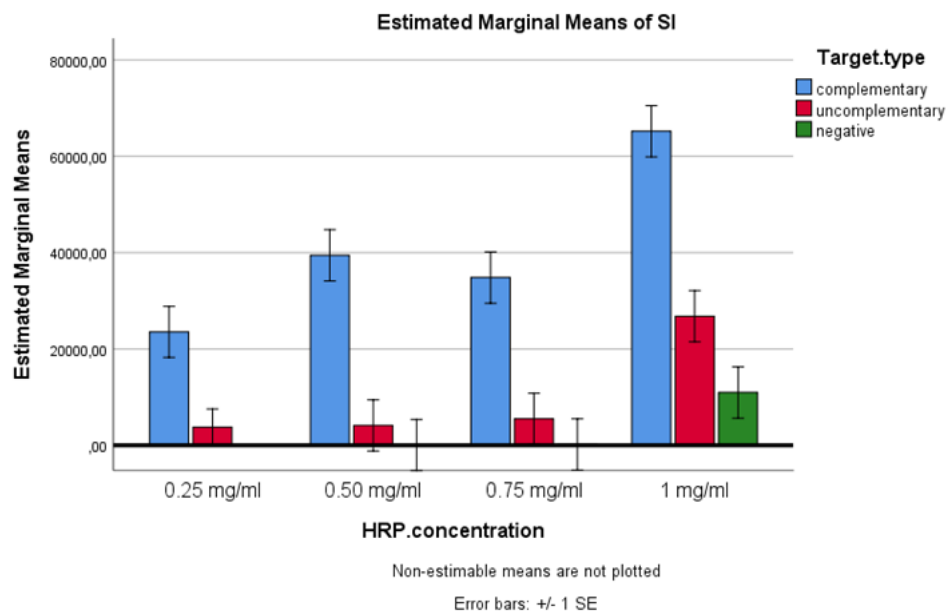
Figure 3.6 *Signal Intensity (SI) for different HRP concentrations 0.25 mg/mL, 0.50 mg/mL, 0.75 mg/mL and 1 mg/mL on LFA. A two-way ANOVA was done to examine the effect of HRP concentrations and target types on SI. There was a significant main effect of the HRP concentrations on SI, $F_{(3, 25)} = 15.10$, $p = .001$.*

Table 3.6 Tests of Between-Subjects Effects (Dependent Variable: SI)

Source	Type III Sum of Squares	df	Mean Square	F	Sig.
HRP concentration	3832897740.349	3	1277632580.116	15.075	.000***
Target type	9957828701.130	2	4978914350.565	58.747	.000***
HRP.concentration * Target.type	629426569.467	5	125885313.893	1.485	.230^{ns}

R Squared = ,865 (Adjusted R Squared = ,811)

3.1.1.1.4. Effect of Different Duration of TMB loading

There was just one significant main effect observed for target types $F_{(2,24)} = 51$, $p < .001$. As shown in the Figure 3.7 and Table 3.7 complementary target had dramatically higher SI (M= 35726,5628) than did uncomplimentary (M= 10441,5580) and negative target (M= 64,2689). Moreover, this was a quite large difference (Partial Eta Squared = .81). On the other hand, there was no significant difference in terms of the duration of TMB loading $F_{(3,24)} = 51$, $p = 1,243$. However, 24h or overnight conditions (12-14h) were preferred for dye loading of MCM-41 in recent studies because it was accepted as a proper time for maximum loading capacity of MCM-41 scaffolding (Climent, Martínez-Máñez, Sancenón, Marcos, Soto, Maquieira, Amorós, *et al.*, 2010) (Kachbouri, Mnasri, Elaloui, & Moussaoui, 2018). Hence, 24h loading was preferred for the duration of TMB loading.
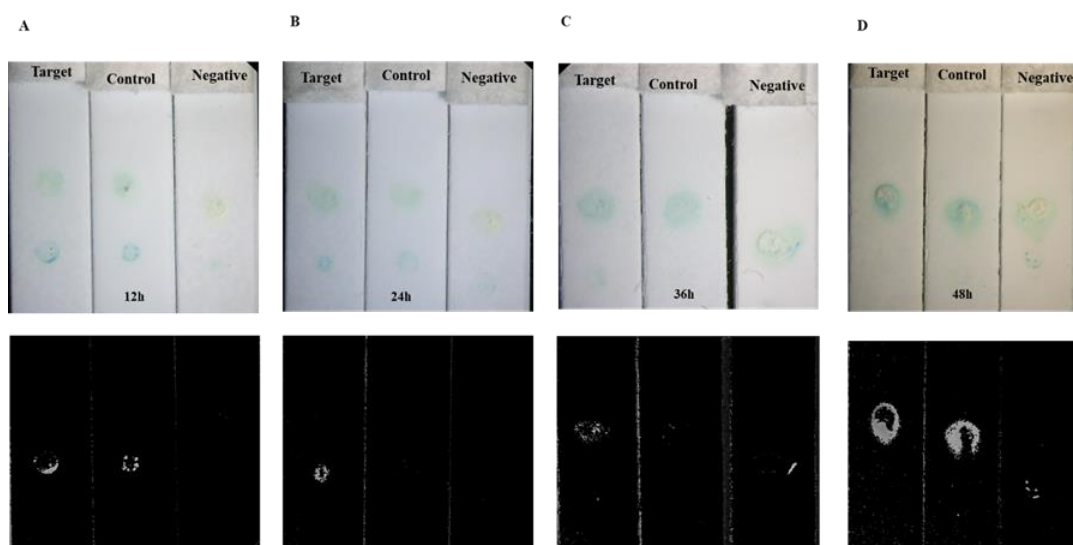
Figure 3.7 Effect of four different TMB loading time on LFA. SiNPs were loaded with 5mM of TMB. Probe capped SiNPs were placed on LFA platforms. (1.5% H_2O_2, 1 mg/mL of HRP and RT). Target (including complementary sequence), Control (composed of uncomplimentary sequence) were applied to LFAs. Instead of nucleic acids, water and 1.5% H_2O_2 was applied as negative. A) The colorimetric response on LFA after 12h TMB loading B) The colorimetric response on LFA after 24h TMB loading C) The colorimetric response on LFA after 36h TMB loading D) The colorimetric response on LFA after 48h TMB loading

Table 3.7 Descriptive statistics of given data set for different loading times of TMB (Dependent Variable: SI)

Target type	TMB loading time	Mean	Std. Deviation	N
complementary	12h	30132,4350	13938,86564	3
	24h	29765,8217	4709,34130	3
	36h	36041,7137	5491,59597	3
	48h	46966,2810	9736,48506	3
	Total	35726,5628	10713,70887	12
uncomplementary	12h	4687,0597	3955,52098	3
	24h	14027,6870	19509,73975	3
	36h	11241,5490	9575,77076	3
	48h	11809,9363	10986,29733	3
	Total	10441,5580	11130,63530	12
negative	12h	16,2597	14,08205	3
	24h	81,9903	30,83045	3
	36h	119,1690	150,84099	3
	48h	39,6567	63,70684	3
	Total	64,2689	82,37218	12
Total	12h	11611,9181	15796,13938	9
	24h	14625,1663	16313,02686	9
	36h	15800,8106	16855,77145	9

48h	19605,2913	22381,96814	9
Total	15410,7966	17485,31666	36
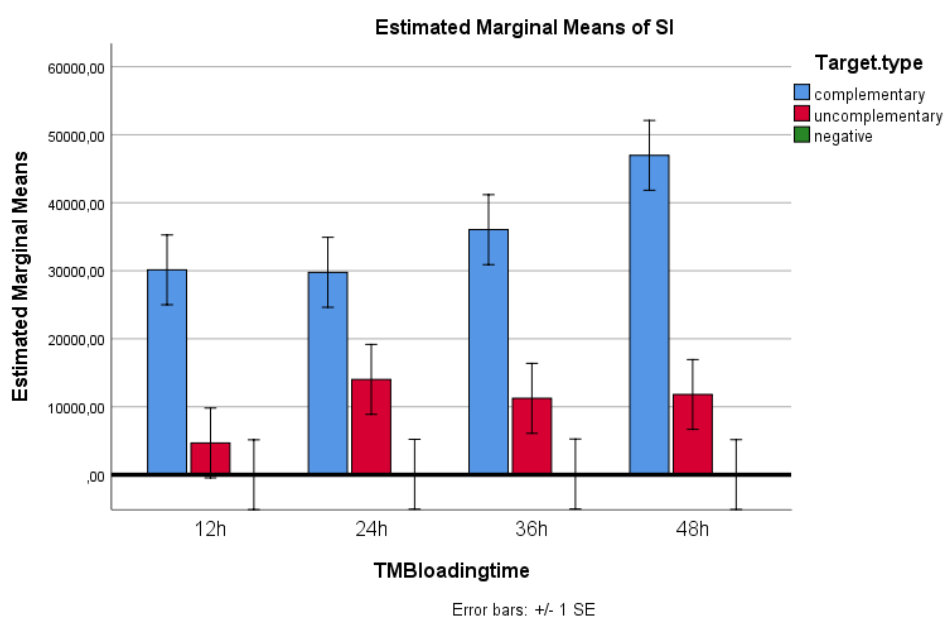
Figure 3.8 Signal Intensity (SI) for different durations (12h,24h,36h,48h) for TMB loading on LFA with probe capped SiNPs. A two-way ANOVA was planned that interpret the effect of TMB loading time and target types on SI. There was a nonsignificant main effect of the dye loading time on SI, F (3,24) = 51, p = 1,243.

Table 3.8 Tests of Between-Subjects Effects (Dependent Variable: SI)

Source	Type III Sum of Squares	df	Mean Square	F	Sig.	Partial Eta Squared
Target type	8075275222,158	2	4037637611,079	50,995	,000***	,810
TMB loading time	295151306,785	3	98383768,928	1,243	,316[ns]	,134
Target type* TMB loading time	430094318,737	6	71682386,456	,905	,508[ns]	,185

3.1.1.1.5. Effect of Different Duration of Silanization

In this part of experiment, MCM-41 was functionalized with 3-aminopropyltriethoxysilane (APTS) under different durations (1.5h, 3h, 4.5h). This process was necessary for capping mesopores with oligonucleotide probes and entrapping TMB inside. During APTES reaction, negatively charged probes interacts with partially positively charged aminopropyl groups (in neutral pH) on the surface of nanoparticle. As a result of this electrostatic interaction, pores of silica nanoparticles was blocked by probes (Climent, Martínez-Máñez, Sancenón, Marcos, Soto, Maquieira, Amorós, *et al*., 2010). A recent study also reported the use of aminated nanoparticles for the interaction with oligonucleotide probes via electrostatic interaction for detecting a specific mutation in β-thalassemia (Ercan, Ozalp, & Tuna, 2017).
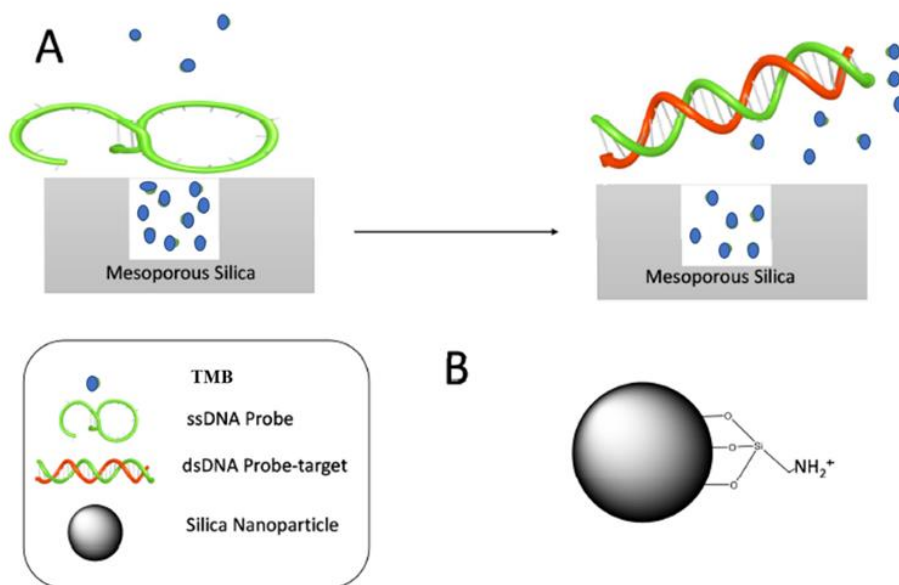
Figure 3.9 Schematic illustration of A) Silanization process, B) Amino-functionalized SiO2 NPs

(Ercan et al., 2017)

Two-way ANOVA was managed to compare the effect of silanization time on SI after 1.5h, 3h and 4.5h of silanization. There was a significant effect of silanization time on signal intensity (SI) at the $p<.05$ level for the three conditions $F_{(2, 18)} = 10,738$, $p = ,001$. Post hoc comparisons depending on the Tukey HSD test showed that the SI for the 4.5h of silanization (M = 23604,797, SD = 2322,644) was significantly different than the 3h of silanization (M = 14708,186, SD = 2322,644) and 1.5h of silanization (M = 8459.59, SD = 2322,644). However, 4.5h of silanization results gave background signal in control. This was probably because of the extended time of silanization which causes multilayer formation in the surface (Howarter & Youngblood, 2006). Considering inefficient APTES reaction due to multilayer formation after 4.5 h of silanization process, mesopores were assumed to not capped with oligonucleotide probes accurately. So that, dye leakage could expected for both control and negative samples. However, it was only seen in control. This was probably the similar reason

in the case of excess TMB. When the duration of silanization was long, interaction between the APTES molecules and control targets destroyed the electrostatic interaction so TMB was released. Furthermore, incomplete functionalization of the surface by amino groups can also create problem like It was seen in 1h of silanization. Leakage of blue dye was observed for both control and negative target. Planned comparisons revealed that, 3h of silanization was convenient for the rest of the experiment.
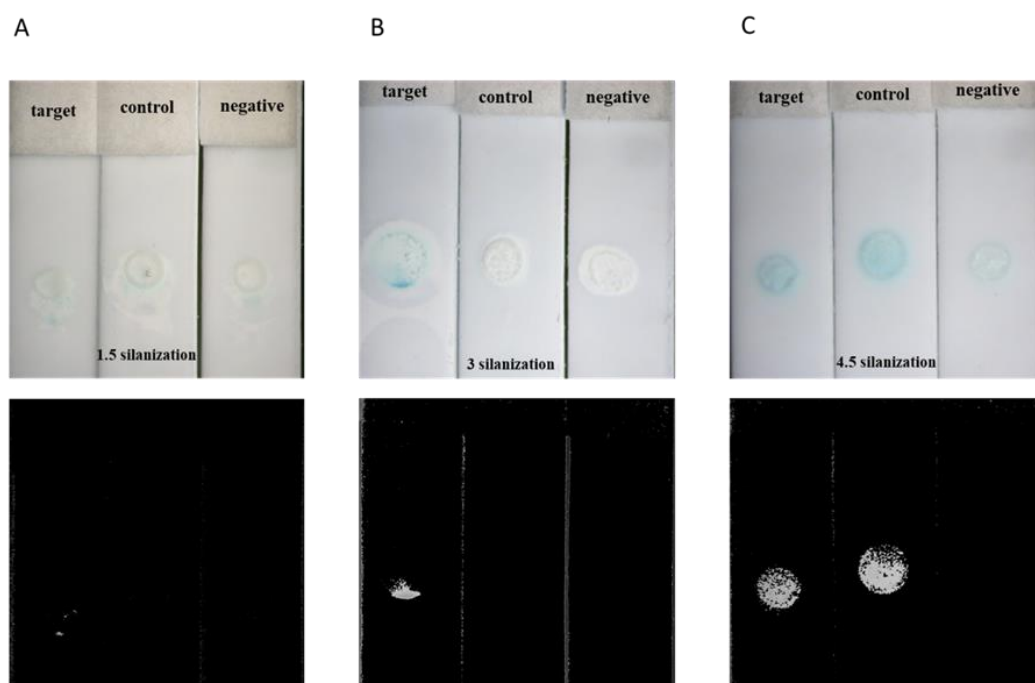
Figure 3.10 Effect of three different silanization time on LFA. SiNPs were loaded with 5mM of TMB. SiNPs closed with probe were placed on LFA set up. (RT, 1 mg/mL of HRP ,1.5% H_2O_2). Target (complementary part), Control (uncomplementary part) were administered to LFAs. Instead of nucleic acids, water and 1.5% H_2O_2 was applied as negative. A) SiNPs were prepared with 1.5 hours silanization B) SiNPs were prepared with 3 hours silanization C) SiNPs were prepared with 4 hours silanization.

Table 3.9 Descriptive statistics of given data set for different silanization times (Dependent Variable: SI)

Silanization.time	Target.type	Mean	Std. Deviation	N
1.5h	complementary	23775,6013	13314,16555	3
	uncomplementary	1158,5327	1030,33896	3
	negative	444,6403	630,63746	3
	Total	8459,5914	13293,92620	9
3h	complementary	44105,9483	3278,80084	3
	uncomplementary	18,6093	32,23231	3
	negative	,0000	,00000	3
	Total	14708,1859	22109,19388	9
4.5h	complementary	46048,8867	8565,95119	3
	uncomplementary	24709,3423	13194,91875	3
	negative	56,1617	97,27486	3
	Total	23604,7969	21428,56723	9
Total	complementary	37976,8121	13397,68346	9
	uncomplementary	8628,8281	13765,48852	9
	negative	166,9340	381,78967	9
	Total	15590,8581	19651,32896	27
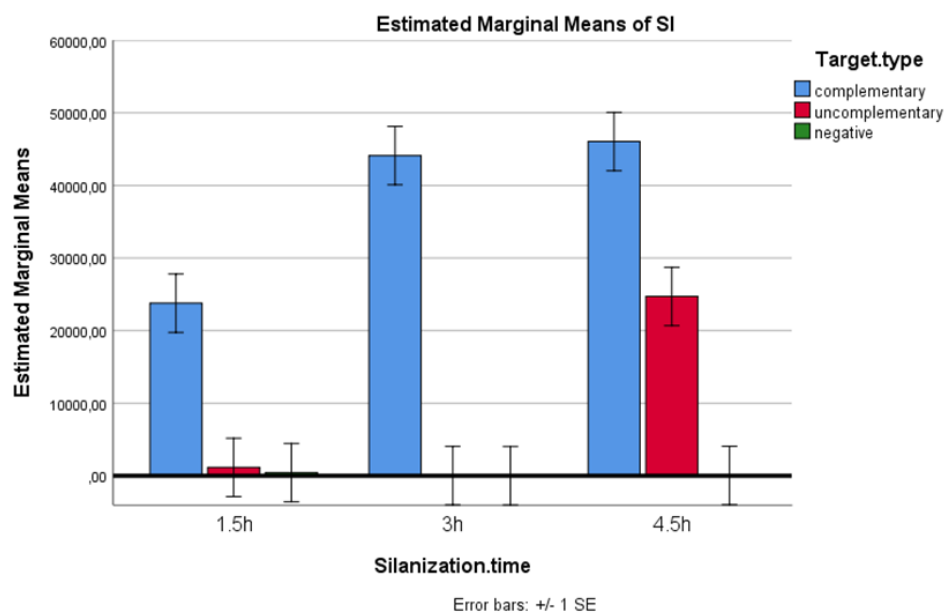
Figure 3.11 The bar graph of SI was reached from SiNPs which was prepared with 1.5 hours, 3 hour and 4.5 hours silanization. Althoug 4.5h silanization gave meaningful result compared to other times, control target produced background signal.

Table 3.10 Tests of Between-Subjects Effects (Dependent Variable: SI)

Source	Type III Sum of Squares	df	Mean Square	F	Sig.	Partial Eta Squared
Silanization time	1042715603,313	2	521357801,656	10,738	,001**	,544
Target.type	7087484098,767	2	3543742049,383	72,988	,000**	,890
Silanization.time* Target.type	1036405786,807	4	259101446,702	5,337	,005**	,543

R Squared = ,913 (Adjusted R Squared = ,874)

3.1.1.1.6. Effect of Different Concentrations of Oligonucleotides

In this part of study, necessary amount of oligonucleotide probes were tried to be optimized to block pores. 0 μM,100 μM and 200 μM probe concentrations were chosen in order to understand pore closing mechanism better. For 0 μM probe, mesapores were not capped and as It was assumed TMB went out from pores.

Although there was no significant difference between 100 μM and 200 μM probe concentrations (two-way ANOVA, P>0.05, n=2), 100 μM was selected as probe concentration for capping pores because it provided high specificity compared to other concentrations. In other words, when SiNPs capped with 100 μM oligonucleotide probe , there was no background signal on LFAs called control and negative. On the other hand, 200 μM probe concentration gave backgroung signal in control LFA since

residual value of TMB dye might cause this undesirable blue color (Climent, Martínez-Máñez, Sancenón, Marcos, Soto, Maquieira, Amorós, *et al*., 2010). Therefore, it was obtained from these experiments that a concentration of 100 μM oligonucleotide was near the optimal concentration to cover mesopores.
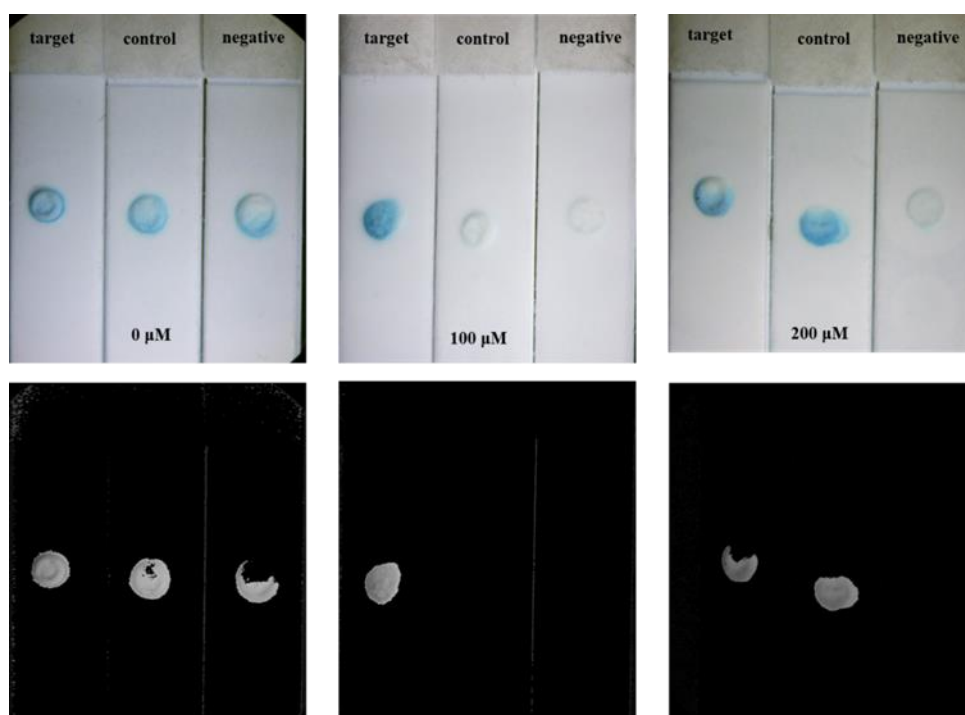
Figure 3.12 Result of LFA in which SiNPs were capped with 0 μM, 100 μM, and 200 μM of oligonucleotide probes. ([TMB] = 5 mM, 1.5 % H_2O_2, 1 mg/mL of HRP and 37 ℃)

Table 3.11 Descriptive statistics of given data set for different concentration of probe (Dependent Variable: SI)

Different concentration of probes	Target.type	Mean	Std. Deviation	N
0 (μM)	complementary	58471,0250	7642,64909	2
	uncomplementary	47137,4230	14402,02282	2
	negative	21547,4910	22895,62260	2
	Total	42385,3130	21076,68329	6
100 μM	complementary	55237,2930	8431,76895	2
	uncomplementary	,0000	,00000	2
	negative	,0000	,00000	2
	Total	18412,4310	28772,57761	6
200 μM	complementary	46040,7310	2734,71002	2
	uncomplementary	30441,4385	43050,69518	2
	negative	24776,3025	35038,98302	2
	Total	33752,8240	26734,40879	6
Total	complementary	53249,6830	7789,06209	6
	uncomplementary	25859,6205	29481,16834	6
	negative	15441,2645	22260,56171	6
	Total	31516,8560	26237,79858	18
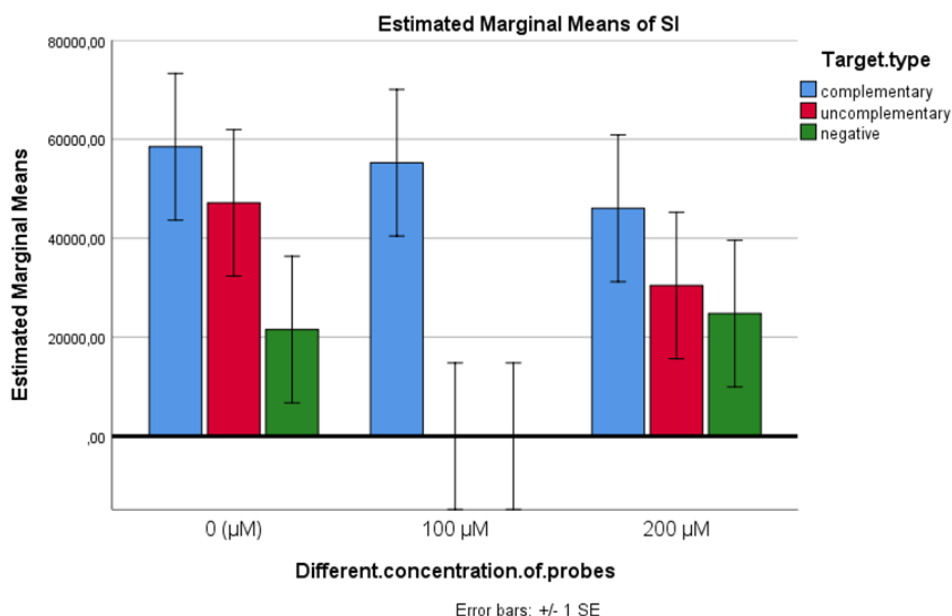
Figure 3.13 The bar graph of SI on LFAs in which SiNPs were prepared with 0uM, 100uM, and 200uM of oligonucleotide probes. 100 uM oligonucleotide probe was preferred because of its specific signal.

3.1.1.1.7. Effect of Different pH

A two-way ANOVA was performed to compare the impact of pH on SI in pH:5, pH:7, pH:9 conditions. A significant main effect was obtained for pH value, $F(2,18) = 4,976$, $p = ,019$. pH:5 had significantly higher SI (M = 57287,26) than did both pH:7 (M = 10677,30) and pH:9 (M = 16,61). This was a moderate difference (Partial Eta Squared =, 36). In addition, TUKEY HSD showed that SI was significantly different pH:5 and pH:7, Mdiff = 15548,662, 95% CI [-4500,741, - 26596,582], p = .008. In one study, pH 7.5 was selected for the controlled delivery of fluorescein with oligonucleotide-capped silica nanoparticle (Climent, Martínez-Máñez, Sancenón, Marcos, Soto, Maquieira, & Amorós, 2010). Also, Ercan *et al*., 2017 also used PBS with pH 7.4 for loading silica nanoparticle with fluorescein to detect single nucleotide

mutation of thalassemia. Nevertheless, PBS pH 5 was added into TMB-H₂O₂ solution to generate blue color when HeLa cells were used (Maji, Mandal, Nguyen, Borah, & Zhao, 2015). This study showed that pH 5 was optimal for detection of the target as given. Thus, pH:5 was selected for the rest of the experiments.
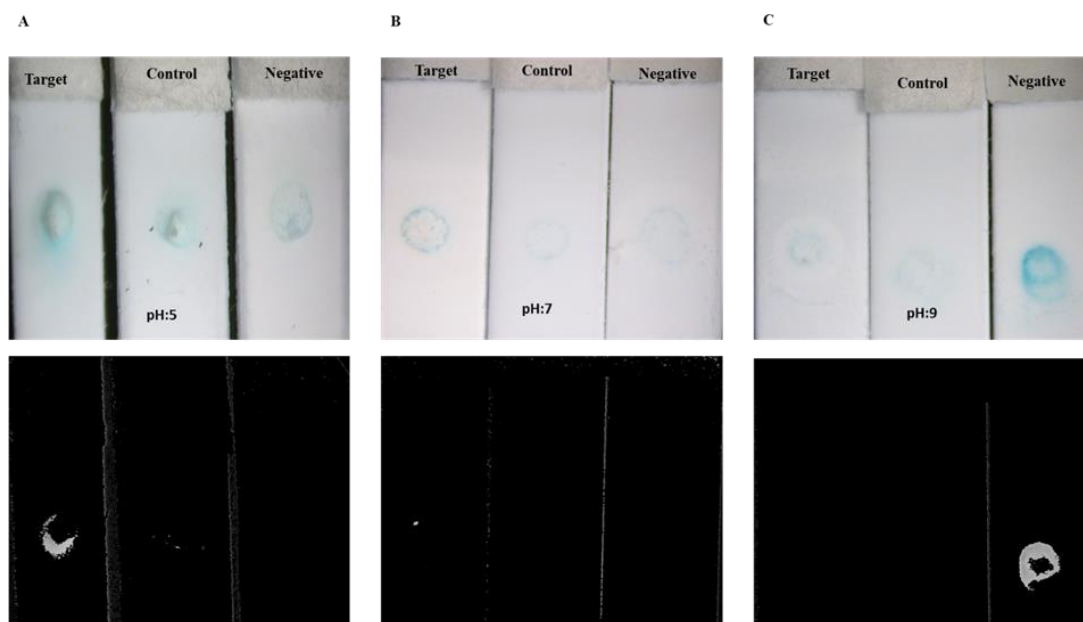
Figure 3.14 Effect of three different pH(5,7,9) on LFA. SiNPs were loaded with 5mM of TMB. Probe capped SiNPs were placed on LFA platforms. (1.5 % H₂O₂, 1 mg/mL of HRP and RT). Target (known as complementary sequence), Control (called as uncomplimentary sequence) were applied to LFAs. Instead of nucleic acids, water, and 1.5 % H₂O₂ was applied as negative. A) pH:5 B) pH:7 C) pH:9

Table 3.12 Descriptive statistics of given data set for different pH (Dependent Variable: SI)

different.ph	Target.type	Mean	Std. Deviation	N
pH:5	complementary	57287,2577	8888,30544	3
	uncomplementary	381,1700	263,65994	3
	negative	69,5940	79,06757	3
	Total	19246,0072	28875,63076	9
pH:7	complementary	10677,2983	1809,86171	3
	uncomplementary	344,3807	414,53951	3
	negative	70,3573	85,51383	3
	Total	3697,3454	5318,14093	9
pH:9	complementary	16,6093	28,76821	3
	uncomplementary	276,0453	313,76282	3
	negative	19099,6240	32207,32921	3
	Total	6464,0929	18686,15306	9
Total	complementary	22660,3884	26764,30123	9
	uncomplementary	333,8653	295,10331	9
	negative	6413,1918	18704,63268	9
	Total	9802,4819	20501,81535	27
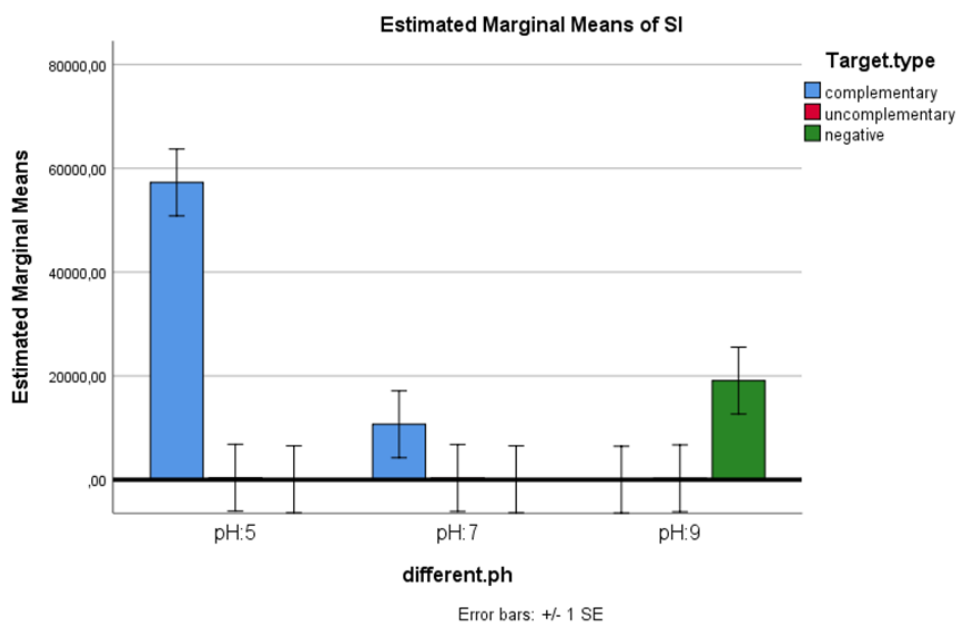
Figure 3.15 The effect of different pH values (5,7,9) on Signal Intensity (SI) with probe capped SiNPs. A two-way ANOVA was planned that conduct the effect of pH value on SI. There was a significant main effect of the pH value on SI, F (2,18) = 4,976, p = ,019

Table 3.13 Tests of Between-Subjects Effects (Dependent Variable: SI)

Source	Type III Sum of Squares	df	Mean Square	F	Sig.	Partial Eta Squared
different.ph	1238379325,577	2	619189662,789	4,976	,019**	,356
Target.type	2398209731,323	2	1199104865,662	9,636	,001***	,517
different.ph * Target.type	5051958540,576	4	1262989635,144	10,150	,000***	,693

R Squared = ,795 (Adjusted R Squared = ,704)

3.1.1.2. Optimization of Lateral Flow Assay Platform

3.1.1.2.1. Flow Rate Through Nitrocellulose Membrane

Selecting lateral flow membrane type is important for experiment design in terms of reliabilty, consistency and specificity. So that, which membrane type can be used was decided in this section. Nitrocellose membranes are classified according to flow times. So different nitrocellulose membranes which means different flow times were compared in this part of study. Flow times were selected as 75,120 and 240 seconds per 4 centimeters of membranes. Table 3.14 summarized the details about membrane types.

Table 3.14 Details about membrane types (Hi-Flow TM Plus Membranes And SureWick ® Pad Materials, n.d.)

Membrane	Capillary Flow Time Specification** (sec/4 cm)	Flow Rate	Sensitivity
HF240	240	Slowest	Most sensitive
HF180	180		
HF135	135		
HF120	120		
HF090	90		
HF075	75	Fastest	Least sensitive

According to two-way ANOVA, the main effect of target type was significant, $F_{(2,18)} = 316,409$, $p < .01$, as was the main effect of membrane type, $F_{(2,18)} = 25,364$, $p < .01$. The interaction of these two factors was also significant, $F_{(4,18)} = 13,741$, $p < .01$. HF075 was not preferred because of its low specific result. It was expected since HF075 is generally preferred when specificity is not a big concern. On the other hand, both HF120 and HF240 gave specific signal with target but SI of HF240 is higher than HF120. TUKEY HSD test also demonstrated that there was a significant difference

between HF120 and HF240 (P= .013, n=3). HF240 gave the highest signal that is probably because of its flow rate. Slow flow rate could allow efficient hybridization of probes and target so that almost all TMB can interact with HRP and produce blue color. Moreover, HF240 provided high sensivity compared to other membrane types (Hi-Flow TM Plus Membranes And SureWick ® Pad Materials, n.d.).
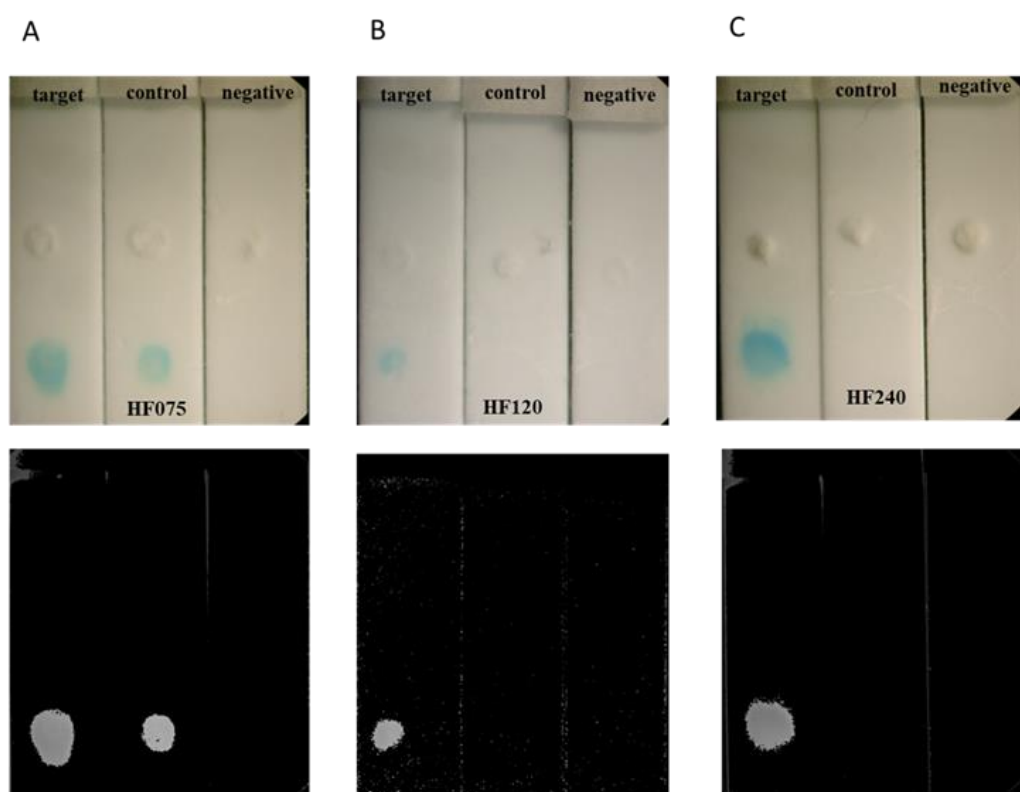
Figure 3.16 The images of LFAs with different nitrocellulose membranes: HF075, HF120 and HF240. ([TMB] = 5 mM, 1.5 % H_2O_2, 1 mg/mL of HRP and 37 ℃)

Table 3.15 Descriptive statistics of given data set for different type of membrane (Dependent Variable: SI)

	Target.type	Mean	Std. Deviation	N
75HF	complementary	91430,0853	6341,45642	3
	uncomplimentary	45277,2413	18740,07212	3
	negative	8,5780	7,94281	3
	Total	45571,9682	40804,46937	9
120HF	complementary	62970,7057	6220,62478	3
	uncomplimentary	119,3630	142,48999	3
	negative	93,9940	33,58790	3
	Total	21061,3542	31585,61381	9
240HF	complementary	91723,4570	7579,25398	3
	uncomplimentary	3,4017	5,89186	3
	negative	36,8220	35,29649	3
	Total	30587,8936	46008,01757	9
Total	complementary	82041,4160	15449,32738	9
	uncomplimentary	15133,3353	24472,91682	9
	negative	46,4647	45,05054	9
	Total	32407,0720	39702,39779	27
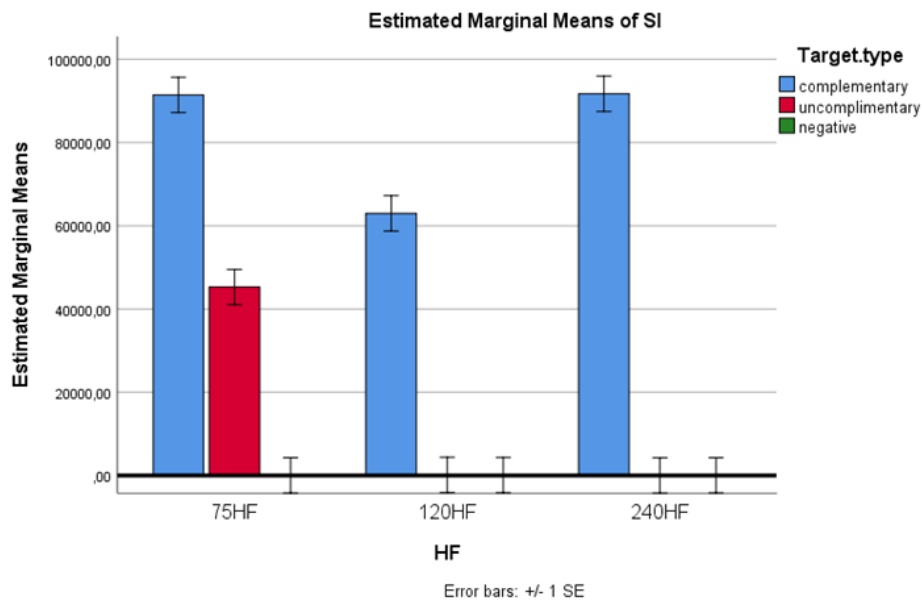
Figure 3.17 The effect of different membrane types on Signal Intensity (SI) with probe capped SiNPs. According to a two-way ANOVA, there was a significant main effect of the membrane types on SI, F (2,18) = 25,364, p = .000. 240 HF was selected as a membrane type because of its high specificity.

Table 3.16 Tests of Between-Subjects Effects (Dependent Variable: SI)

Source	Type III Sum of Squares	df	Mean Square	F	Sig.	Partial Eta Squared
Target type	34282430907,497	2	17141215453,748	316,409	,000***	,972
HF	2748142931,828	2	1374071465,914	25,364	,000***	,738
HF * Target type	2977579478,371	4	744394869,593	13,741	,000***	,753

R Squared = ,976 (Adjusted R Squared = ,966

3.1.1.2.2. Distance between Silica Nanoparticle and HRP

The position of nanoparticle and HRP is important for the efficiency of the test. Ratio 2:1 was selected for distance parameter due to the results of previous studies. SiNPs were placed on 4 mm,6mm and 8mm away from sample pad and then HRP 2mm, 3mm and 4mm below SiNPs respectively. When SiNPs is farther from the sample loading part of the strip, more interaction time could be possible (Posthuma-Trumpie, Korf, & Van Amerongen, 2009). So, It was expected that better hybridization might occur when SiNPs placed 6mm or 8mm below sample pad than did 2mm,which could result with high signal intensity. According to two-way ANOVA, a significant main effect was obtained for different distances, $F (2,9) = 22,92$, p= .000. SiNPs placed 6mm below sample pad gave higher SI (M= 67191,18) than 4mm (M= 26001,73) and 8mm (M= 38866,61). TUKEY HSD test also demostrated that the SI was similar for 4mm and 8 mm M_{diff} = 835,953, 95% CI [-2649,482, 4321,387], p = .601; however it was higher for 6mm compared to 4mm M_{diff} =-8586,821, 95% CI [-12072,256, -5101,387], p = . 000 and significantly higher for 6mm compared to 8mm M_{diff} =-9422,774, 95% CI [-12908,209, -5937,339], p = . 000.

HRP position was also important because it is the converter of H_2O_2/TMB to visible blue color. When HRP was placed away from TMB, and therefore sample pad; due to the direction of lateral flow assay, the reaction time and the concentration of H_2O_2 reached to HRP decreased. As a result, the probability of H_2O_2 molecules encountered with HRP can low (Fung *et al*., 2009). So as it was seen in 8mm-4mm distance, HRP might not have long enough reaction time to convert H_2O_2/TMB into blue signal.

The data suggested that SiNPs could be placed 6mm below sample pad and then HRP might located 3mm below SiNPs.
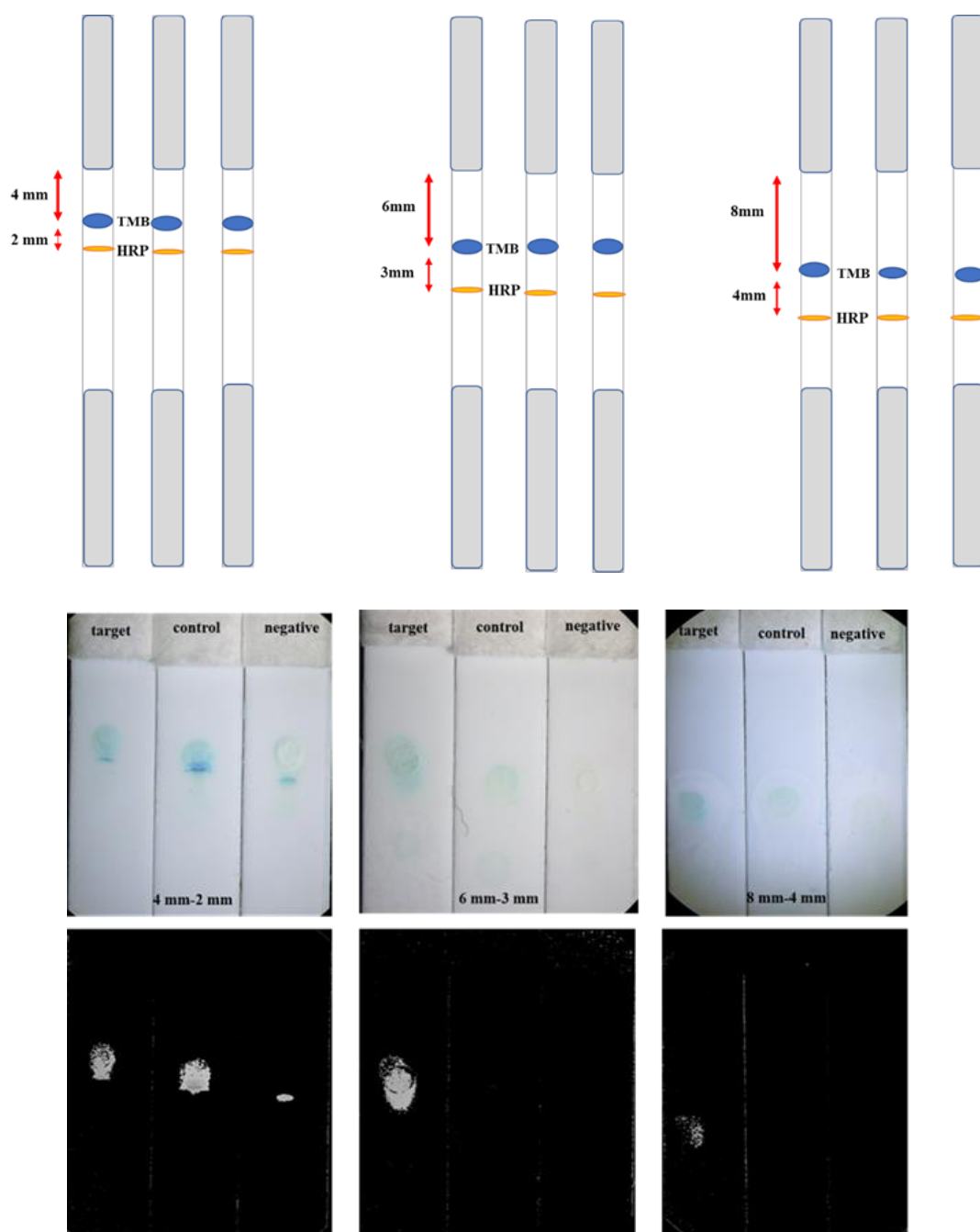
Figure 3.18 Effect of three different distance between SiNPs and HRP on LFA. SiNPs were loaded with 5mM of TMB. Probe capped SiNPs were placed on LFA platforms. (1.5% H_2O_2, 1 mg/mL of HRP and RT). Target (including complementary sequence), Control (composed of uncomplimentary sequence) were applied to LFAs. Instead of nucleic acids, water, and 1.5% H_2O_2 was applied as negative. A) 4mm-2mm B) 6mm-3mm C) 8mm-4mm

Table 3.17 Descriptive statistics of given data set for different distance (Dependent Variable: SI)

Distance	Target.type	Mean	Std. Deviation	N
4mm-2mm	complementary	26001,7330	2214,53116	2
	uncomplementary	3751,4100	422,18659	2
	negative	11722,3005	2923,73593	2
	Total	13825,1478	10217,37144	6
6mm-3mm	complementary	67191,1790	6976,70724	2
	uncomplementary	38,4565	10,20143	2
	negative	6,2715	8,86924	2
	Total	22411,9690	34825,87718	6
8mm-4mm	complementary	38866,6130	1337,42601	2
	uncomplementary	56,9295	14,72974	2
	negative	44,0425	44,67430	2
	Total	12989,1950	20053,49533	6
Total	complementary	44019,8417	19139,51441	6
	uncomplementary	1282,2653	1921,92247	6
	negative	3924,2048	6180,33366	6
	Total	16408,7706	22910,74414	18
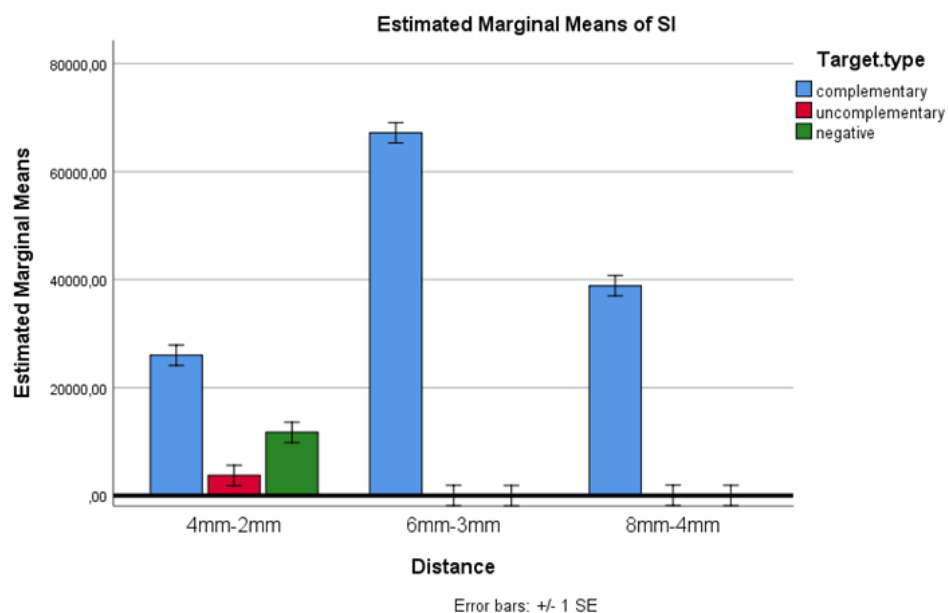
Figure 3.19 The effect of different distance between silica nanoparticle and HRP on Signal Intensity (SI) with probe capped SiNPs. According to a two-way ANOVA, there was a significant main effect of distance on SI, F (2,18) = 22.92, p = .000. 6mm-3mm distance was preferred because of its high specificity and SI.

Table 3.18 Tests of Between-Subjects Effects (Dependent Variable: SI)

Source	Type III Sum of Squares	df	Mean Square	F	Sig.	Partial Eta Squared
Distance	326441969,486	2	163220984,743	22,919	,000**	,836
Target.type	6882280736,479	2	3441140368,240	483,184	,000**	,991
Distance * Target.type	1650518471,508	4	412629617,877	57,939	,000**	,963

R Squared = ,993 (Adjusted R Squared = ,986)

3.1.1.3. The sensitivity of Silica Nanoparticle-Based Lateral Flow Assay

3.1.1.3.1. Limit of Detection for Synthetic Targets

The presence of target oligonucleotide is critical for this study since target hybridized with probe and it induced opening pores and releasing TMB. Moreover, it was found that the delivery of dye is relative to concentration of target (Climent, Martínez-Máñez, Sancenón, Marcos, Soto, Maquieira, & Amorós, 2010).

As illustrated Figure 3.21, It could be realized that the releasing of the TMB is proportional to the target concentration. The proper release was seen at a target concentration of 35 μM. For higher concentrations than 35 μM, TMB releasing could partially inhibited, it was probably due to excess target adsorbed onto the nanoparticle's surface, which resulted in partial pore blocking (Climent, Martínez-Máñez, Sancenón, Marcos, Soto, Maquieira, Amorós, *et al*., 2010). Until 7.5 μM of synthetic targets, TMB continued releasing.
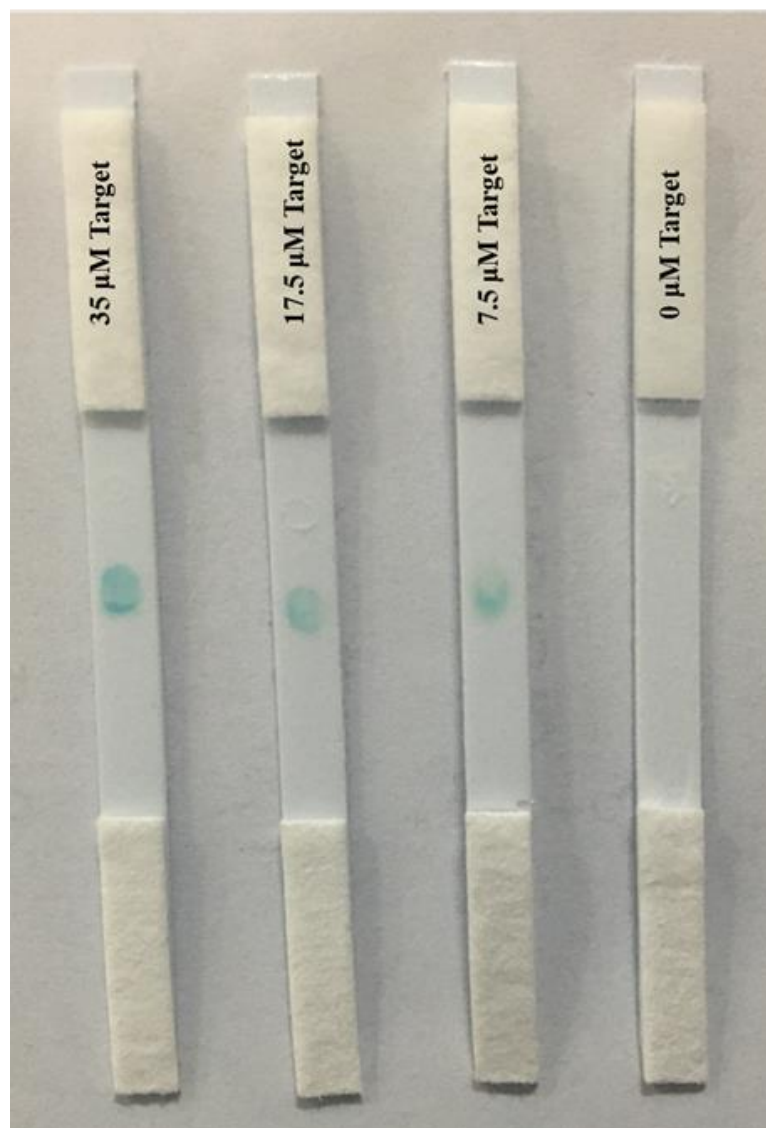
Figure 3.20 The overall image of LFAs, gradual concentration of synthetic complementary Target (35 μM, 17.5 μM, 7.5 μM and 0 μM). ([TMB] = 5 mM, 1.5 % H_2O_2, 1 mg/mL of HRP and 37℃

Table 3.19 Descriptive statistics of given data set for different concentration of targets (Dependent Variable: SI)

Target concentration	Mean	Std. Deviation	N
35 µM Target	51227,2868	11377,89932	4
17.5 µM Target	22833,2413	13734,42664	4
7.5 µM Target	19714,0362	3052,12920	4
0 µM Target	19,6475	18,12809	4
Total	23448,5529	20529,34194	16
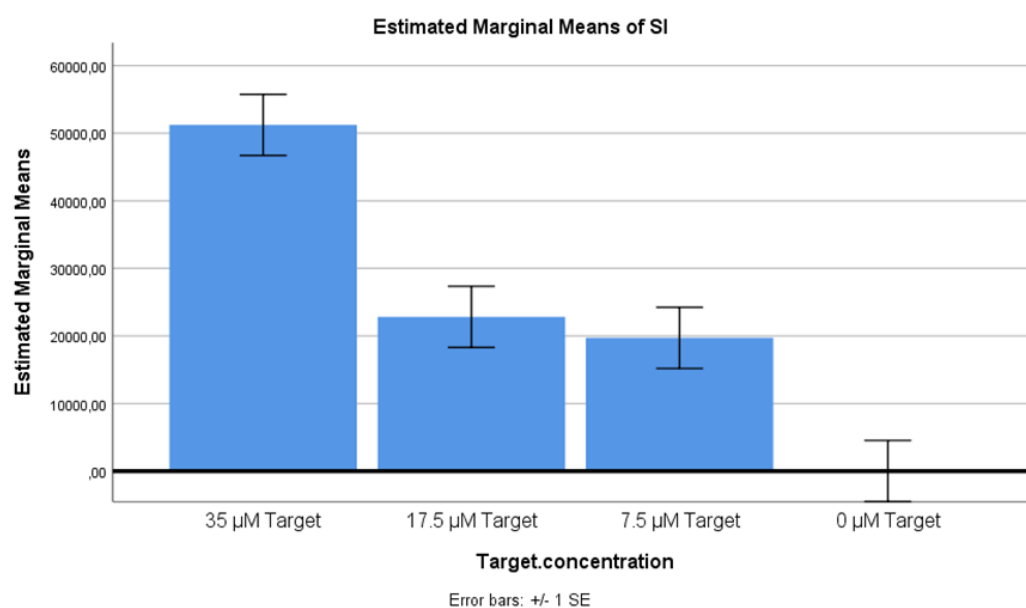
Figure 3.21 The result of different concentration of target on Signal Intensity (SI) with probe capped SiNPs. According to a one-way ANOVA, there was a significant main effect of target concentration on SI, $F_{(3,16)} = 21.75$, $p = .000$.

Table 3.20 Tests of Between-Subjects Effects (Dependent Variable: SI)

Source	Type III Sum of Squares	df	Mean Square	F	Sig.	Partial Eta Squared
Target concentration	5339587542,34 8	3	1779862514,11 6	21,74 5	,000** *	,845

R Squared = ,845 (Adjusted R Squared = ,806)

CHAPTER 4

CONCLUSION

An assay for detecting the presence of *eaeA* gene from synthetic target samples was developed with the help of probe-gated silica nanoparticles. In this study, SiNPs were loaded with TMB and then its mesopores were covered with probe oligonucleotides. After all these processes, it was placed on LFA, and immobilized by membrane. Later, HRP was placed LFA just below SiNPs. Target amplicon with complementary sequence to probes and H_2O_2 were sent from sample pad. As a result, cargo molecule, 3,3′,5,5′-Tetramethylbenzidine (TMB), was liberated and oxidized by HRP-H_2O_2. Hence, a blue color had occurred on LFA and its signal intensity was measured by image J software and statistically analyzed by SPSS program.

First of all, colorimetric reaction parameters were optimized. 1.5 % H_2O_2 was preferred for proper signal propagation on LFAs although there was no significant difference between the concentration of H_2O_2. 5 mM TMB was selected instead of 10 mM because of its high specificity even if, 10 mM produced high signal intensity compared to other ones. 1mg/mL HRP concentration was found proper for this colorimetric reaction since it produced statistically higher signal than other HRP concentrations did. Duration of TMB loading on nanoparticle might also be considered as an important issue, however according to our data there was no significant main effect of TMB loading time. Despite the fact that high signal intensity was obtained in 48 h, 24 h duration was chosen because of its high selectivity. Duration of silanization was also another critical concern when the results of different times was thought. 3h silanization gave the most reliable outcome since there was little background on LFA composed of control and negative target. When efficient pore

coverage was considered, concentration of probe oligonucleotide was another essential point. 100 μM oligonucleotide was near the ideal concentration for pore blockage since its high specificity and signal. Although, the most common buffer systems used in similar experiments in literature was 1X PBS with pH: 7.4, our data provided convenient result when pH was 5.

Then, lateral flow assay platform was optimized. Flow membrane type was important for experiment design in terms of speed and specificity. 240HF was chosen because it was more sensitive than other membrane types (75HF and 120HF) although its flow rate was the slowest. Distance ratio of SiNPs and HRP on LFA was arranged 6mm-3mm for higher signal and sensivity. Sensitivity of SiNPs based LFAs was demonstrated with synthetic targets. Minimum 7.5 μM of synthetic targets was sensed on LoD experiments of the test.

For future studies, better performing probe-gated biosensors could be developed in order to prevent leakage problem seen on LFA consist of control and negative target. Furthermore, the selectivity and signal intensity of LFA assays rely so heavily on many factors such as type and amount of sample, its condition, pH of buffer, concentration of target and probe, interaction forces between the probe and target oligonucleotides. For our study, these challenges could be partially overcomed in controlled conditions. However, the performance of LFA test may be affected in real sample situation. Hence, conditions of assay can be improved to obtain blue color with also PCR product of *eaeA* gene. To handle this issue, future studies may focus on to generate LFA devices more practicle, optimized, shorter incubation steps, quantitative results formation.

REFERENCES

Amerongen, A. Van, Veen, J., Arends, H. A., & Koets, M. (2018). Lateral Flow Immunoassays. In *Handbook of Immunoassay Technologies*. https://doi.org/10.1016/B978-0-12-811762-0.00007-4

Arora, P., Sindhu, A., Dilbaghi, N., & Chaudhury, A. (2011). Biosensors as innovative tools for the detection of food borne pathogens. *Biosensors and Bioelectronics*, *28*(1), 1–12. https://doi.org/10.1016/j.bios.2011.06.002

Bahadır, E. B., & Sezgintürk, M. K. (2016). Lateral flow assays: Principles, designs and labels. *TrAC - Trends in Analytical Chemistry*, *82*, 286–306. https://doi.org/10.1016/j.trac.2016.06.006

Center for Disease Control and Prevention. (2018). *Escherichia coli (E. coli) Factsheet*. (September). https://doi.org/10.1128/AAC.01103-16

Cepeda-Molero, M., Berger, C. N., Walsham, A. D. S., Ellis, S. J., Wemyss-Holden, S., Schüller, S., … Fernández, L. Á. (2017). Attaching and effacing (A/E) lesion formation by enteropathogenic E. coli on human intestinal mucosa is dependent on non-LEE effectors. *PLoS Pathogens*, *13*(10), 1–23. https://doi.org/10.1371/journal.ppat.1006706

Chen, Y., Fu, Q., Xie, J., Wang, H., & Tang, Y. (2019). Development of a high sensitivity quantum dot-based fluorescent quenching lateral flow assay for the detection of zearalenone. *Analytical and Bioanalytical Chemistry*, *411*(10), 2169–2175. https://doi.org/10.1007/s00216-019-01652-1

Climent, E., Martínez-Máñez, R., Sancenón, F. F. F., Marcos, M. D., Soto, J., Maquieira, A., … Martínez-Máñez, R. (2010). Controlled delivery using oligonucleotide-capped mesoporous silica nanoparticles. *Angewandte Chemie (International Ed. in English)*, *49*(40), 7281–7283. https://doi.org/10.1002/anie.201001847

Climent, E., Martínez-Máñez, R., Sancenón, F., Marcos, M. D., Soto, J., Maquieira, A., & Amorós, P. (2010). Controlled delivery using oligonucleotide-capped mesoporous silica nanoparticles. *Angewandte Chemie - International Edition*, *49*(40), 7281–7283. https://doi.org/10.1002/anie.201001847

Donnenberg, M. S., Tacket, C. O., James, S. P., Losonsky, G., Nataro, J. P., Wasserman, S. S., … Levine, M. M. (1993). Role of the eaeA gene in experimental enteropathogenic Escherichia coli infection. *Journal of Clinical Investigation*, *92*(3), 1412–1417. https://doi.org/10.1172/JCI116717

Dwivedi, H. P., & Jaykus, L. A. (2011). Detection of pathogens in foods: The current state-of-the-art and future directions. *Critical Reviews in Microbiology*, *37*(1), 40–63. https://doi.org/10.3109/1040841X.2010.506430

Eltzov, E., Guttel, S., Low Yuen Kei, A., Sinawang, P. D., Ionescu, R. E., & Marks, R. S. (2015). Lateral Flow Immunoassays - from Paper Strip to Smartphone Technology. *Electroanalysis*, *27*(9), 2116–2130. https://doi.org/10.1002/elan.201500237

Ercan, M., Ozalp, V. C., & Tuna, B. G. (2017). Genotyping of single nucleotide polymorphism by probe-gated silica nanoparticles. *Analytical Biochemistry*, *537*, 78–83. https://doi.org/10.1016/j.ab.2017.09.004

Ferreira, T., & Rasband, W. (2012). ImageJ User Guide ImageJ User Guide IJ 1.46r. Retrieved from https://imagej.nih.gov/ij/docs/guide/user-guide.pdf

Fung, K. K., Chan, C. P. Y., & Renneberg, R. (2009). Development of enzyme-based bar code-style lateral-flow assay for hydrogen peroxide determination. *Analytica Chimica Acta*, *634*(1), 89–95. https://doi.org/10.1016/j.aca.2008.11.064

Gao, L., Wu, J., & Gao, D. (2011). Enzyme-controlled self-assembly and transformation of nanostructures in a tetramethylbenzidine/horseradish peroxidase/H 2O 2 system. *ACS Nano*, *5*(8), 6736–6742.

https://doi.org/10.1021/nn2023107

Gao, X., Xu, L.-P., Zhou, S.-F., Liu, G., & Zhang, X. (2014). Recent Advances in
Nanoparticles-based Lateral Flow Biosensors. *American Journal of Biomedical Sciences*, *6*(1), 41–57. https://doi.org/10.5099/aj140100041

Godambe, L. P., Bandekar, J., & Shashidhar, R. (2017). Species specific PCR based
detection of Escherichia coli from Indian foods. *3 Biotech*, *7*(2), 1–5.
https://doi.org/10.1007/s13205-017-0784-8

Havelaar, A. H., Cawthorne, A., Angulo, F., Bellinger, D., Corrigan, T., Cravioto,
A., … Kuchenmüller, T. (2013). WHO Initiative to Estimate the Global Burden
of Foodborne Diseases. *The Lancet*, *381*(5), S59.
https://doi.org/10.1016/S0140-6736(13)61313-6

Hi-Flow ᵀᴹ Plus Membranes And SureWick ® Pad Materials. (n.d.). Retrieved from
http://www.scienman.com.tw/download/millpore/Millipore_HiFlo_SureWickpb
1267en00.pdf

Howarter, J. A., & Youngblood, J. P. (2006). Optimization of silica silanization by
3-aminopropyltriethoxysilane. *Langmuir*, *22*(26), 11142–11147.
https://doi.org/10.1021/la061240g

Iqbal, S. S., Mayo, M. W., Bruno, J. G., Bronk, B. V, Batt, C. A., & Chambers, J. P.
(2000). *A review of molecular recognition technologies for detection of
biological threat agents*. *15*, 549–578.

Kachbouri, S., Mnasri, N., Elaloui, E., & Moussaoui, Y. (2018). Tuning particle
morphology of mesoporous silica nanoparticles for adsorption of dyes from
aqueous solution. *Journal of Saudi Chemical Society*, *22*(4), 405–415.
https://doi.org/10.1016/j.jscs.2017.08.005

Kumar, B. K., Raghunath, P., Devegowda, D., & Kumar, D. V. (2011). *Development
of monoclonal antibody based sandwich ELISA for the rapid detection of
pathogenic Vibrio parahaemolyticus in seafood*. (January).

https://doi.org/10.1016/j.ijfoodmicro.2010.12.030

Lathwal, S., & Sikes, H. D. (2016). Assessment of colorimetric amplification methods in a paper-based immunoassay for diagnosis of malaria. *Lab on a Chip*, *16*(8), 1374–1382. https://doi.org/10.1039/c6lc00058d

Law, J. W. F., Mutalib, N. S. A., Chan, K. G., & Lee, L. H. (2014). Rapid metho ds for the detection of foodborne bacterial pathogens: Principles, applications, advantages and limitations. *Frontiers in Microbiology*, *5*(DEC), 1–19. https://doi.org/10.3389/fmicb.2014.00770

Maji, S. K., Mandal, A. K., Nguyen, K. T., Borah, P., & Zhao, Y. (2015). Cancer cell detection and therapeutics using peroxidase-active nanohybrid of gold nanoparticle-loaded mesoporous silica-coated graphene. *ACS Applied Materials and Interfaces*, *7*(18), 9807–9816. https://doi.org/10.1021/acsami.5b01758

Mak, W. C., Beni, V., & Turner, A. P. F. (2016). Lateral-flow technology: From visual to instrumental. *TrAC - Trends in Analytical Chemistry*, *79*, 297–305. https://doi.org/10.1016/j.trac.2015.10.017

Makvana, S., & Krilov, L. R. (2015). Escherichia coli Infections. *Pediatrics in Review*, *36*(4), 167–171. https://doi.org/10.1542/pir.36-4-167

Mckee, M. L., & O'Brien, A. D. (1996). Truncated enterohemorrhagic Escherichia coli (EHEC) O157:H7 intimin (EaeA) fusion proteins promote adherence of EHEC strains to HEp-2 cells. *Infection and Immunity*, *64*(6), 2225–2233.

Pan, R., Jiang, Y., Sun, L., Wang, R., Zhuang, K., Zhao, Y., … Man, C. (2018). Gold nanoparticle-based enhanced lateral flow immunoassay for detection of Cronobacter sakazakii in powdered infant formula. *Journal of Dairy Science*, 1–9. https://doi.org/10.3168/jds.2017-14265

Pennington, H. (2010). Escherichia coli O157. *The Lancet*, *376*(9750), 1428–1435. https://doi.org/10.1016/S0140-6736(10)60963-4

Posthuma-Trumpie, G. A., Korf, J., & Van Amerongen, A. (2009). Lateral flow (immuno)assay: Its strengths, weaknesses, opportunities and threats. A literature survey. *Analytical and Bioanalytical Chemistry*, *393*(2), 569–582. https://doi.org/10.1007/s00216-008-2287-2

Priyanka, B., Patil, R. K., & Dwarakanath, S. (2016). A review on detection methods used for foodborne pathogens. *Indian Journal of Medical Research*, *144*(September), 327–338. https://doi.org/10.4103/0971-5916.198677

Quesada-González, D., Jairo, G. A., Blake, R. C., Blake, D. A., & Merkoçi, A. (2018). Uranium (VI) detection in groundwater using a gold nanoparticle/paper-based lateral flow device. *Scientific Reports*, *8*(1), 8–15. https://doi.org/10.1038/s41598-018-34610-5

Quesada-González, D., & Merkoçi, A. (2015). Nanoparticle-based lateral flow biosensors. *Biosensors and Bioelectronics*, *73*, 47–63. https://doi.org/10.1016/j.bios.2015.05.050

Singh, A., Poshtiban, S., & Evoy, S. (2013). Recent advances in bacteriophage based biosensors for food-borne pathogen detection. *Sensors (Switzerland)*, *13*(2), 1763–1786. https://doi.org/10.3390/s130201763

Song, C., Liu, C., Wu, S., Li, H., Guo, H., Yang, B., … Liu, Q. (2016). Development of a lateral fl ow colloidal gold immunoassay strip for the simultaneous detection of Shigella boydii and Escherichia coli O157 : H7 in bread , milk and jelly samples. *Food Control*, *59*, 345–351. https://doi.org/10.1016/j.foodcont.2015.06.012

Song, S., Zou, S., Zhu, J., Liu, L., & Kuang, H. (2018). Immunochromatographic paper sensor for ultrasensitive colorimetric detection of cadmium. *Food and Agricultural Immunology*, *29*(1), 3–13. https://doi.org/10.1080/09540105.2017.1354358

Ünüvar, S. (2018). Chapter 1 - Microbial Foodborne Diseases. In *Handbook of Food*

Bioengineering. https://doi.org/https://doi.org/10.1016/B978-0-12-811444-5.00001-4

Valderrama, W. B., Dudley, E. G., Doores, S., Catherine, N., Valderrama, W. B., Dudley, E. G., & Doores, S. (2016). *Commercially Available Rapid Methods for Detection of Selected Food-borne Pathogens Commercially Available Rapid Methods for Detection of Selected Food-borne Pathogens*. *8398*. https://doi.org/10.1080/10408398.2013.775567

World Health Organization. (2015). *WHO estimates of the global burden of foodborne diseases: executive summary*. 1–2. https://doi.org/10.1016/j.fm.2014.07.009

Yang, S. C., Lin, C. H., Aljuffali, I. A., & Fang, J. Y. (2017). Current pathogenic Escherichia coli foodborne outbreak cases and therapy development. *Archives of Microbiology*, *199*(6), 811–825. https://doi.org/10.1007/s00203-017-1393-y

Yeni, F., Yavaş, S., Alpas, H., & Soyer, Y. (2016). Most Common Foodborne Pathogens and Mycotoxins on Fresh Produce: A Review of Recent Outbreaks. *Critical Reviews in Food Science and Nutrition*, *56*(9), 1532–1544. https://doi.org/10.1080/10408398.2013.777021

Zhang, Hailong. (2014). *Lateral flow test strip based on colloidal selenium immunoassay for rapid detection of melamine in milk , milk powder , and animal feed*. 1699–1707.

Zhang, Hongwei, Ma, L., Ma, L., Hua, M. Z., Wang, S., & Lu, X. (2017). International Journal of Food Microbiology Rapid detection of methicillin-resistant Staphylococcus aureus in pork using a nucleic acid-based lateral fl ow immunoassay. *International Journal of Food Microbiology*, *243*, 64–69. https://doi.org/10.1016/j.ijfoodmicro.2016.12.003

Zhang, Q., Li, M., Guo, C., Jia, Z., Wan, G., Wang, S., & Min, D. (2019). Fe3O4Nanoparticles Loaded on Lignin Nanoparticles Applied as a Peroxidase

Mimic for the Sensitively Colorimetric Detection of H2O2. *Nanomaterials*, *9*(2), 210. https://doi.org/10.3390/nano9020210

Zhao, S., Wang, S., Zhang, S., Liu, J., & Dong, Y. (2018). State of the art: Lateral flow assay (LFA) biosensor for on-site rapid detection. *Chinese Chemical Letters*, *29*(11), 1567–1577. https://doi.org/10.1016/j.cclet.2017.12.008

Zhao, X., Lin, C. W., Wang, J., & Oh, D. H. (2014). Advances in rapid detection methods for foodborne pathogens. *Journal of Microbiology and Biotechnology*, *24*(3), 297–312. https://doi.org/10.4014/jmb.1310.10013

APPENDICES

A. BUFFERS AND SOLUTIONS

Tryptic Soy Broth (TSB)

17 g of casein, 3 g of soya peptone, 5 g of NaCl and 2.5 g of K_2HPO_4 were weighed and completely dispersed in 1L of dH_2O. pH of the solution was arranged to 7.3 with 1M of NaOH and 1M of HCl. Suspension was sterilized with autoclave at 121oC for 15 minutes. The broth was stored at 4 oC. it was taken 30 minutes from fridge before usage of TSB.

Tryptic Soy Agar (TSA)

17 g of casein, 3 g of soya peptone, 5 g of NaCl, 2.5 g of K_2HPO_4 and 15 g of agar were weighed and completely dispersed in 1 L of dH_2O. pH of solution was arranged to 7.3 by the help of 1M of NaOH and 1M of HCl. Suspension was sterilized with autoclave at 121oC for 15 minutes. After autoclaving done and temperature was around 80 oC, it was distributed into sterile plates under laminar hood. To check sterility, at least one of plate was carried on 37 °C and waited at RT. TSA was used immediately.

Luria-Bertani Broth (LBB)

10 g of tryptone, 5 g of yeast extract and 10 g of NaCl were weighed and solved in 1L of dH_2O. pH was arranged to 7.0 with 1M of NaOH and 1M of HCl. The medium was sterilized with autoclave for 150 minutes at 121°C. The broth was kept at 4 °C.

Luria-Bertani Agar (LBA)

10 g of tryptone, 5 g of yeast extract 10 g of NaCl and 10 g of agar were weighed and dispersed in 1L of dH_2O . pH was arranged to 7.0 with 1M of NaOH and 1M of HCl. Mixture was autoclaved for 150 minutes at 121℃. After autoclaving done and temperature was around 80 ℃, it was filled into sterile plates under laminar hood. To check sterility, at least one of plate was carried on 37℃ and waited at RT. LBA was freshly used.

Dulbecco's Phosphate Buffered Saline (Ca++ Mg++ Free PBS)

200 mL of dH_2O was prepared in a suitable container. 2 g of NaCl, 50 mg of KCl, 360 mg of Na2HPO4, 60 mg of KH2PO4 were added to the solution. pH was adjusted to 5.4 by adding 5M HCl. dH_2O was added until volume is 0.25 L.

TMB Stock Solution (1M)

0.240 g of 3,3′,5,5′-Tetramethylbenzidine (TMB) was weighed and dispersed in 1 mL of dimethyl sulfoxide (DMSO).

TMB Working Solutions

100 μL of TMB stock solution and 400 μL of DMSO were mixed and 0.2M of TMB solution was prepared. 250 μL of TMB stock solution and 250 μL of DMSO were mixed and 0.5M of TMB solution was prepared.

HRP solutions

0.25 mg of HRP was weighed and dissolved in 250 μL of filtered MilliQ for 1mg/mL. 0.1 mg of HRP was weighed and dissolved in 200 μL of filtered for 0.5 mg/mL

H_2O_2 solution

Stock solution was 30.0% w/v hydrogen peroxide. 1mL of a 1.5%, 2.5%, 3.5%,4.5%,5.5% H_2O_2 were prepared from stock solution. 1.5% w/v H_2O_2 contained 1.5g of solute for 100 mL of solution. So 1 mL target solution contain 0.015g H_2O_2 .

%w/v= (msolute /Vsolution.).100 => Vsolution=(msolute/%w/v).100 =>) 0.015g/30g/mL).100

$V_{SOLUTION}$=0.05 mL=50 uL. (50 uL stock solution and 950 uLdH_2O)

Other concentrations were prepared according to these calculations.

B. SEQUENCES OF PRIMERS, PROBES, TARGETS

Table B.1 Sequences of primers

Primers	*Sequence*
eae A forward primer:	*CAATTTTTCAGGGAATAACATTG*
eae A reverse primer:	*AAAGTTCAGATCTTGATGACATTG*

Table B.2 Sequences of probes

Probe Oligonucleotides	Sequence
Probe	TCAAGAGTTGCCCATCCTGCAGCAA

Table B.3 Sequences of targets

Target Oligonucleotides	Sequence
Target	TTGCTGCAGGATGGGCAACTCTTGA
Control (strephyg2_F)	TCTGTCGCTGTCTCAAGCAG

C. SEQUENCES OF TARGET eaeA GENE

Target gene:

>U32312.1 Escherichia coli 0157:H7 intimin (eaeA) gene, partial cds, and upstream ORF gene, complete cds

GGATCCCATCGTTTCGTCTAAATATATCCATAATCATTTTATTTAGAGGG
AGGGAGGGGGGAAGTCTAACTAACGTCAATTTTTCAGGGAATAACATTG
CTGCAGGATGGGCAACTCTTGAGCTTCTGTAAATATAAATTTAATTAAGA
GAAAATACAATGTCATCAAGATCTGAACTTTTATTAGAAAAATTTGCAGA
AAAAATTGGTATTGGATCTATTTCATTTAATGAAACAGATTGTGTTCTT
TTGCTATTGATGAAATTTATTATATTTCGTTATCTGATGCCAATGACGAAT
ATATGATGATTTATGGTGTCTGTGGGAAATTCCCGACAGATAACTCTAAC
TTCGCTCTTGAGATTTTGAATGCAAACTTATGGTTTGCAGAGAATGGTGG
CCCATATCTGTGCTATGAGGCTGGAGCACAATCGCTGTTGTTAGCGTTAC
GTTTCCCTCTCGATGATGCTACCCCTGAAAAACTCGAGAATGAAATAGA
AGTCGTTGTTAAGTCAATGGAAAACCTGTATTGGTATTACATAATCAGG
GAATAACATTAGAAAACGAACATATGAAAATAGAGGAAATCAGTTCAA
GCGACAATAAACATTATTACGCCGGAAGATAAAATCCGATCTATTAATA
TAATTTATTTCTCATTCTAACTCATTGTGGTGGAGCCATACATGATTACTC
ATGGTTGTTATACCCGGACCCGGCACAAGCATAAGCTAAAAAAAACATT
GATTATGCTTAGTGCTGGTTTAGGATTGTTTTTTTATGTTAATCAGAATTC